NASA TECHNICAL NOTE

NASA TN D-2868

NASA TN D-2868

ARC-JET THRUSTOR FOR SPACE PROPULSION

by Lewis E. Wallner and Joseph Czika, Jr.

Lewis Research Center
Cleveland, Ohio

NATIONAL AERONAUTICS AND SPACE ADMINISTRATION • WASHINGTON, D. C. • JUNE 1965

NASA TN D-2868

ARC-JET THRUSTOR FOR SPACE PROPULSION

By Lewis E. Wallner and Joseph Czika, Jr.

Lewis Research Center
Cleveland, Ohio

NATIONAL AERONAUTICS AND SPACE ADMINISTRATION

For sale by the Clearinghouse for Federal Scientific and Technical Information
Springfield, Virginia 22151 – Price $3.00

CONTENTS

ARC-JET THRUSTOR FOR SPACE PROPULSION

by Lewis E. Wallner and Joseph Czika, Jr.

Lewis Research Center

26647

SUMMARY

The arc-jet thrustor represents an engine for potential space applications requiring a specific impulse in the range from 1000 to 2000 seconds. As such it was originally thought that missions for the engine would fit somewhere between those suitable for the high thrust chemical and the very low thrust ion propulsion systems. The considerable effort expended to develop the arc thrustor has resulted in operation in the power range from 1 to 200 kilowatts, at specific impulse levels between 1000 and 2000 seconds, and for continuous running as long as 500 hours with overall efficiency up to 55 percent. Progress has been made on many of the early operating problems such as electrode-erosion, nozzle-cooling, and propellant-feed systems. In addition, theories have been advanced to explain, at least partially, the electric-arc operation. In substance then, the thermal arc-jet thrustor is now fairly well developed. Because of several factors unrelated to impulse and efficiency levels, however, the mission application of the arc thrustor is somewhat doubtful at the present time. These factors, for the larger arc-jet thrustor, include biological shielding, hardware availability, excessive electric generator weight, and reliability, for example.

author

INTRODUCTION

Excessive mission time and large vehicle weight for a given payload are two difficult considerations that confront scientists in performance of more ambitious space projects. Two methods for gaining relief from these problems are the use of higher energy propellants and engine types capable of operating at much greater impulse levels. The numerous propulsive principles that have been proposed range from the resistojet, with an impulse level somewhat higher than that available chemically, to the photon rocket, which may have a potential specific impulse in excess of 100 000 seconds (refs. 1 and 2).

Each propulsive principle has its enthusiastic proponents, which sometimes make the selection of advanced engine types something less than scientific. Important factors to consider in sponsoring a new engine development range from the likely improvement in performance with the advanced thrustor to the potential difficulty in perfecting all the required subsystems. Analytical estimates of improved performance to be gained from electric propulsion are plentiful in the early literature (refs. 1 and 3 to 5). The attendant problems associated with the required systems, however, did not become manifest until considerable expenditure of time and effort was made. During the interim between the arc-jet proposals in the time period from 1957 to 1959 and today, it has become clear that chemical propulsion not only represents a system in being but also a rapidly improving one. The large increase in conventional rocket-vehicle performance over a 10-year period (refs. 6 and 7) is an important consideration not to be overlooked in any comparison analysis.

Alternately, mission-analysis studies can quickly lead to the requirement for impulse levels higher than those of a chemical rocket for the attainment of the more ambitious space journeys (ref. 8). The thermal-arc-jet thrustor represents an engine type in the specific-impulse range from 1000 to 2000 seconds. Advanced arc thrustors have been proposed in specific-impulse levels to 10 000 seconds; the practical limitations have not yet been determined. For the purpose of distinction, the arc jet, which operates in the 1000- to 2000-second range, is termed "thermal"; propellant acceleration occurs by adding heat to a gas and then converting the thermal energy to velocity by expanding the gas in a conventional nozzle. The arc-type thrustor in the high specific-impulse range is termed "high-specific-impulse thrustor"; its accelerating mechanism is the combination of a thermal and an electromagnetic process. Use of the thermal arc jet has been proposed for missions in cislunar space by many analysts in the past several years (refs. 3, 5, and 9). The higher impulse and resultant improved payload ratios compared with chemical rockets have encouraged considerable research and development work. This has led to a marked improvement in the areas of arc-jet-thrustor efficiency, erosion, lifetimes, etc. The present study is an effort to assess the status of the arc thrustor and to examine the current usefulness of this engine as a space-propulsive device in the light of present-day technology.

The Lewis Research Center has sponsored many research contracts on arc-thrustor sizes between 1- and 200-kilowatt power levels, engine components, and system integration. The subject report is particularly timely at present because of two factors: First, most of the original thrustor-operating problems have been solved. Further useful work, therefore, requires definition of mission application, power level, and engine type. Second, the recent large increase in electric-generator weight at the higher power levels will force a reexamination of the relative position of many electric-propulsion systems.

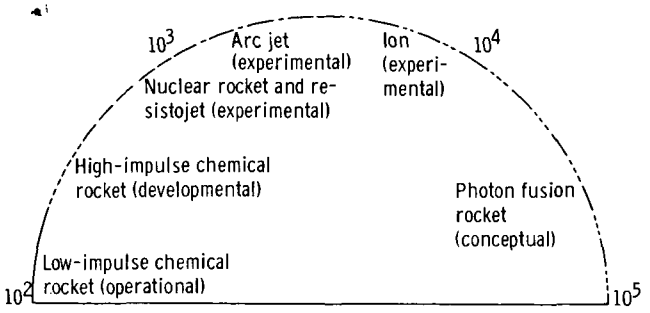

Figure 1. - Impulse spectrum for various types of space-propulsion methods.

Interest in the electric arc for heating gases to extreme temperatures dates back to the turn of the century; however, the recent increased interest in arc heating was created by the need for aerodynamic simulation in small high-speed tunnels in the 1950 time period (ref. 10). Because the specific impulse of a propulsive device can be related to temperature, which at the core of an electric-arc discharge may be as high as 50 000° K (ref. 11), it was natural that the electric arc was looked upon as a means of heating a propellant considerably above the 6000° F range available chemically. The desirability of covering the entire impulse spectrum was first based on the belief that, because of the wide variety of missions, it would be necessary to develop many propulsive systems - hence, an obvious justification for working on arc-jet thrustors (fig. 1). Now, some 5 years after the early mission studies and after considerable development work, the propulsion designer is better situated to assess the relative merits of the thermal arc jet. It has become abundantly clear that impulse or efficiency are far from adequate descriptions of propulsion-system requirements. Such subjects as hardware availability, power generation, reliability, biological shielding, and engine operating time may outweigh the impulse or efficiency concepts.

PHYSICS OF ARC-JETS

A thermal arc jet converts electrical energy to thermal energy by heat transfer from an arc discharge to a propellant and from thermal energy to directed kinetic energy by an appropriate expansion through a nozzle. Thermal energy in the steady-state arc is produced by Joule heating; that is, electromagnetic forces do work on the charged particles (ions and electrons) that distribute the energy to the inner propellant gas by collisions. The energy in the arc is transferred to the outer propellant gas by diffusion, convection, and conduction. The propellant gas finally undergoes an expansion in order to convert thermal energy into directed kinetic energy.

The processes just described are actually quite complex. For the purpose of a more detailed discussion, the physics of the arc jet can be divided into three conceptual regions:

(1) Thermodynamics of propellants

(2) Aerodynamics of arc-jet flow

(3) Arc-energy transfer modes

With each region is associated an efficiency of energy conversion. Consideration of the thermodynamics of propellants involves the concept of frozen flow and a quantity called the frozen-flow efficiency, which is defined as

$$\eta_f = \frac{\text{Power in fluid available for thrust}}{\text{Power in fluid}}$$

The aerodynamic expansion process in the nozzle involves a quantity called the nozzle efficiency, which is defined as

$$\eta_n = \frac{\text{Thrust power}}{\text{Power in fluid available for thrust}}$$

The energy-injection mechanism of input power to gas power involves a quantity called the arc efficiency, which is defined as

$$\eta_a = \frac{\text{Power in fluid}}{\text{Input power}}$$

(The input power includes not only electric power, but also the power in the inlet gas due to nonzero temperature and pressure storage. At times this may be a sizable portion of the input power). The overall efficiency of the device may be defined as

$$\eta_o = \frac{\text{Thrust power}}{\text{Input power}}$$

thus

$$\eta_o = \eta_a \eta_f \eta_n$$

The efficiencies will be defined in algebraic quantities when needed.

The thermal arc jet can operate in several different modes according to design geometry and arc ambient conditions. Many operating modes can be simplified to analytical models. These can be classified into two general categories, constricted and unconstricted, which refer to the operating mode of the arc. The unconstricted-arc mode is one in which the arc is in a nearly quiescent atmosphere. The constricted-arc mode is one in which the arc is restricted to operate in a specified manner. This can be done by special configurations, fluid forces, electromagnetic forces, or any combination of these. The complex operation of an actual arc jet can easily be made amenable to

solution by the unconstricted-arc model of the arc jet. Strictly speaking, the unconstricted arc cannot exist in this device by virtue of the convective action of the incoming gas, but the approximation can be made and the analyses are generally satisfactory.

THERMODYNAMICS OF PROPELLANTS

In principle, any gas or vapor can be utilized as the propellant in an arc jet. Obviously, some gases have more desirable characteristics than others. Because it appears that the overall efficiency cannot be higher than the frozen-flow efficiency, the latter will serve as a figure of merit (keeping η_{arc} and η_{nozzle} constant) in the comparison of propellants. Other desirable characteristics of propellants include a low stagnation enthalpy (for a given specific impulse) to ensure low heat loading on the engine structure. Although some general trends may be established for desirable propellants, definitive requirements for "good" propellants are subject to the mission to which a particular arc jet may be applied.

The frozen-flow loss is a direct consequence of the failure of atoms, electrons, and ions to recombine within their residence time in the nozzle. If the pressure and stagnation enthalpy are known, the amount of energy vested in ionization and dissociation for a given propellant can be calculated from a Mollier chart (fig. 2, ref. 12), which relates

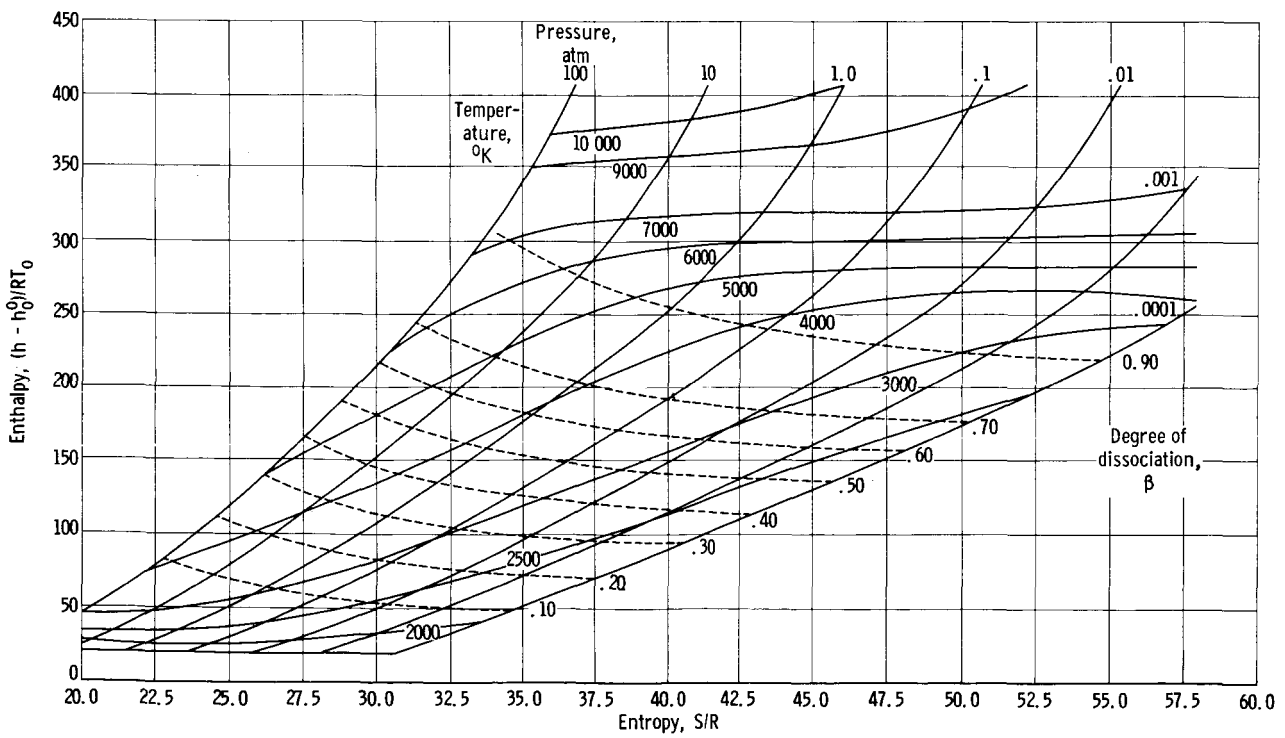

Figure 2. - Mollier chart for hydrogen (ref. 12).

the equilibrium values of the thermodynamic variables. Dissociation and ionization energy not recoverable for propulsion are "frozen" into the flow. The point during an expansion at which an equilibrium flow freezes has been mathematically analyzed by Bray (ref. 13). The Bray criteria show that, in the arc-jet thrustor, under the conditions of uniform, isentropic, one-dimensional flow, freezing takes place at the throat (ref. 14).

In order to develop analytic expressions relating quantities of interest, the assumption of uniform, isentropic, one-dimensional flow is made. The adiabatic energy is used to relate the enthalpies at the plenum and at the nozzle-exit plane

$$h_t = h_o + \frac{V^2}{2}$$

where h_t is the stagnation enthalpy, h_o is the static enthalpy (containing the frozen enthalpy and unused thermal energy), and V is the exit gas velocity. An overall power balance with the arc jet results in $h_t = \eta_a \frac{P}{\dot{m}}$, where P is the total input power (electrical power plus storage gas power), $\dot{m}$ is the mass flow rate, and η_a is the input power to gas power efficiency. The thrust T of the thrustor is given by

$$T = \dot{m}V + (P_E - P_A)A_{ex}$$

where P_E is the pressure at the nozzle exit plane, P_A is the ambient pressure, and A_{ex} is the area of the nozzle exit plane. The specific impulse is given by

$$I_{sp} \equiv \frac{T}{\dot{m}g} = \frac{V}{g} + (P_E - P_A)\frac{A_{ex}}{\dot{m}g}$$

where g is acceleration due to gravity. For simplicity, assume a complete expansion ($P_E = P_A$ and $h_o = h_f$). Then,

$$I_{sp} = \frac{1}{g}\sqrt{2(h_t - h_f)}$$

$$= C\sqrt{h_t - h_f}$$

where C is a constant depending on the units of enthalpy. The frozen-flow efficiency is defined by

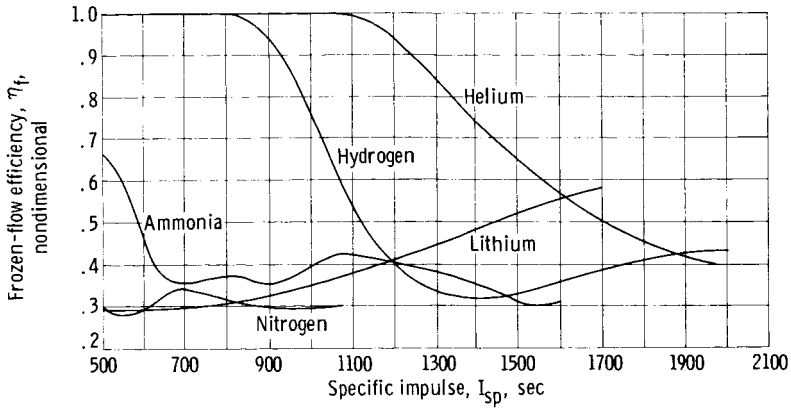

Figure 3. - Theoretical variation of frozen-flow efficiency with specific impulse at pressure of 1 atmosphere.

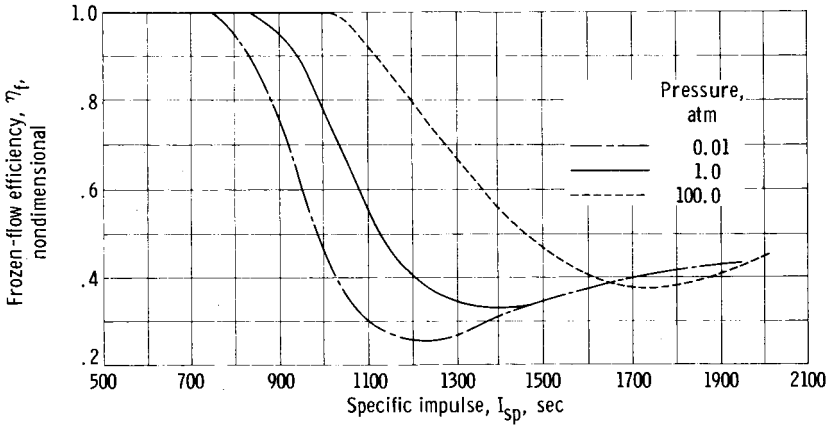

Figure 4. - Theoretical variation of frozen-flow efficiency with specific impulse for hydrogen at various pressures.

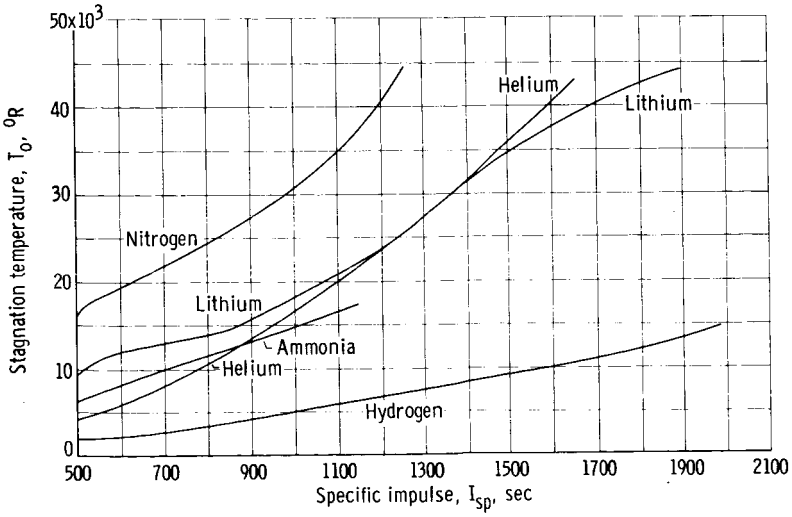

Figure 5. - Theoretical variation of stagnation temperature with specific impulse at pressure of 1 atmosphere.

$$\eta_f = \frac{h_t - h_f}{h_t}$$

thus

$$I_{sp} = C\sqrt{\eta_f h_t}$$

Formulation of the preceding relations has been detailed by Jack (ref. 15) and Schaefer and Ferrante (ref. 16).

The thermal arc jet operates in the range of specific impulse from 1000 to 2000 seconds; gas properties commensurate with this level will be of major interest. Figure 3 (refs. 15 and 16) shows the variation of frozen-flow efficiency with specific impulse for several gases at a pressure of 1 atmosphere. Figure 4 shows the variation of η_f as a function of I_{sp} with pressure for hydrogen. As a general rule, higher pressure increases the frozen-flow efficiency at a given specific impulse for any propellant. Although it appears from figure 3 that a particular propellant may be optimum at a given impulse, other factors must also be weighed. The stagnation temperature as a function of specific impulse for some propellants is shown in figure 5, from which an estimate of the heat load on the engine structure can be obtained. Hence, the practical limitation of thrustor cooling may dictate a propellant other than that determined from frozen-flow considerations. Also, mission requirements such as storability may negate the best propellant based on the curves in figures 3 and 5.

AERODYNAMICS OF PROPELLANTS

Another important consideration of arc-jet physics is the behavior of the fluid flow, especially during the expansion process. Qualitatively, the propellant, after being heated, passes through a decreasing-area channel to accelerate it. At some point, usually the minimum area, the flow will choke (Mach number 1). Downstream of the throat the channel is divergent so the flow is further accelerated. The whole process after heating is called the expansion process. To describe the flow in the arc jet mathematically, the assumption of isentropic expansion is used. Basically, the isentropic condition means that every thermodynamic state in the expansion process is at the same entropy. This is manifest in the condition of reversible adiabatic flow. When the flow is also considered to be frozen, as is in the arc jet, the process is said to be a frozen isentropic expansion, where the ratio of specific heats, is constant. If the flow variables change only with respect to the axial (direction of flow) coordinate, the flow is called

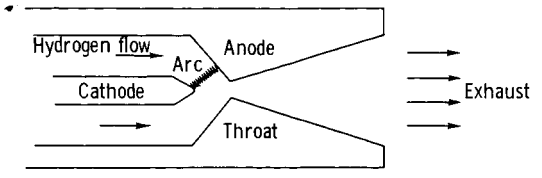

(a) Unconfined arc.

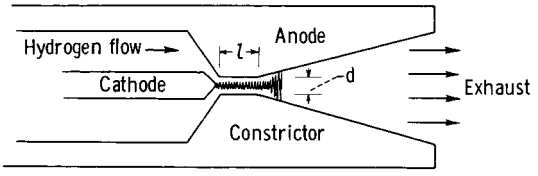

(b) Confined or constricted arc.

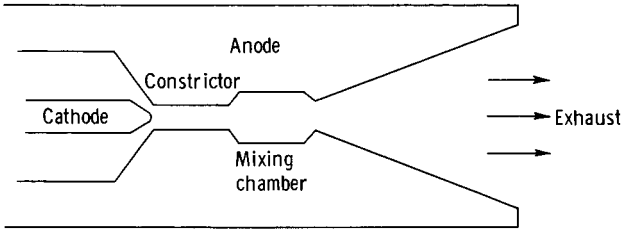

(c) Confined arc with mixing chamber.

Figure 6. - Arc design of arc jet.

one-dimensional. It is expected in the first approximation that the flow in the arc jet can be described by the well-known, one-dimensional, isentropic flow equations (ref. 17).

In reality the flow is not the ideal one-dimensional isentropic process just described. The obvious heat transfer from gas to structure and the presence of wall friction (boundary layer) destroys ideal flow. A measure of the energy loss in these two effects is the nozzle efficiency η_n defined earlier. For nozzles of the size used in medium- and high-power arc jets, the best nozzle efficiencies are expected to be above 90 percent. In the low-power thrustors, the nozzle efficiency may fall to 80 percent.

Energy-Transfer Modes

Another major consideration in an arc-jet device is the mode of energy transfer from the arc to the gas. In general, the thermal arc jet can operate in either an unconstricted- or constricted-arc configuration, the former being the most obvious and historically the first tried. The unconstricted-arc configuration is one in which the arc is free-burning; that is, the arc will strike as it would in a nearly quiescent atmosphere (fig. 6(a)). The constricted-arc configuration is one in which the arc is restricted to operate in a specified manner in the form of special configurations with various parts externally cooled, the use of electromagnetic or fluid forces, or other means; it is largely used in arc-jet propulsion and is shown in figure 6(b). Although details of current designs will be discussed later, for the time being the general features will be delineated. The throat (minimum area) portion of the unconstricted-arc design is replaced by a constant area channel (L/D ratio ≥ 1) called a constrictor. The throat (point at which the flow chokes) is usually at the downstream end of the constrictor. The cathode is a rod with its conical tip very near the constrictor inlet. The arc is forced by the inlet flow to pass down the constrictor and should attach just downstream of the throat. The size of the arc and the mode of arc-electrode attachment differ between the confined

and unconfined arc jet. Even in various designs of the confined arc jet, the arc operation differs, which gives rise to various analytical interpretations of the arc jet.

In order to analyze the energy-transfer mechanisms occurring in arc-jet designs, several models have been proposed. The most obvious approach assumes the propellant to be heated uniformly, in which case, the mechanism of heating is not important. The advantage of this simplification is that it permits the construction of a model of the arc-jet operation in which the previous analyses of the thermodynamics and aerodynamics of propellants are adopted without modification. The model roughly describes the operation of all thermal arc jets; however, the arc jets that seem to perform best for propulsion application are of the constricted-arc design, where heating and flow nonuniformities exist. The aforementioned model inadequately describes these designs. Thus far there have been only two proposed models for the constricted arc that have adequately described the arc heating process; the hot-wire or core-flow theory (refs. 18 and 19) and the Stine-Watson or volumetric-heat-addition theory (ref. 20).

Uniformly Heated Propellant Model

In principle, uniform propellant heat distribution can be obtained by providing a plenum to smooth out any nonuniformities. Such a plenum is downstream of the arc but before the freezing point. In practice, wholly uniform flow is impossible because of heat transfer, boundary-layer growth, and other practical considerations. Nevertheless, the arc can either be unconstricted or constricted. One configuration that utilizes a mixing chamber is shown in figure 6(c), where the mixing chamber is a bulge in the constrictor section.

Some interesting limitations on the performance of the uniformly heated propellant arc-jet model can be deduced from figures 3 to 5 (p. 7). Assume the maximum temperature permitting structural integrity of the engine (for a certain hypothetical cooling design) to be about 6120° R and a stagnation pressure of 1 atmosphere. Figures 3 to 5 show that, for hydrogen under these conditions, the maximum specific impulse is about 1100 seconds and the maximum frozen-flow efficiency is 55 percent. In any physical arc jet designed to approximate the uniformly heated propellant model closely, heat transfer and viscosity would tend to decrease these values.

The basic consideration of both theoretical models of the constricted-arc mode is the construction of a conservation of energy equation for the arc. A simplifying assumption is made at the outset that the only region (or at least the very dominant one) of the arc that heats the gas is the positive column. In general, in the positive column, the energy flux is equal to the rate of generation of that energy. Because energy in the arc is produced by acceleration of charged particles (Joule heating), the rate of energy pro-

duction is σE^2, where σ is the electrical conductivity (assumed to be a function of temperature at a given pressure) and E is the electric field (assumed to be constant). The energy equation is then

$$\sigma E^2 = \text{div } \vec{Q}$$

where $\vec{Q}$ is the heat flux. In general $\vec{Q}$ is composed of heat transfer in three modes: conduction, convection, and radiation. If conduction is assumed to act radially outward from the center of the arc and axially along the arc and convection to act only along the axis, the energy equation in cylindrical coordinates simplifies to

$$\sigma(T)E^2 = P_{rad}(T) - \frac{1}{r}\frac{\partial}{\partial r} rK(T)\frac{\partial T}{\partial r} - \frac{\partial}{\partial z} K(T)\frac{\partial T}{\partial z} + \frac{\partial}{\partial z}(\rho v_z h)$$

where

$P_{rad}(T)$	radiated power (as function of temperature)
$K(T)$	thermal conductivity (as function of temperature)
T	temperature, $T(r, z)$
ρ	gas density
v_z	gas velocity
h	local total enthalpy, $h(r, z)$

The substitution $dS = K(T)dT$ is often made so that the energy equation at a given pressure is

$$\sigma E^2 = P_{rad} - \frac{1}{r}\frac{\partial}{\partial r}\left(r\frac{\partial S}{\partial r}\right) - \frac{\partial^2 S}{\partial z^2} + \frac{\partial}{\partial z}\rho v_z h$$

Each model assumes a different dominant heat-transfer mode by neglecting either a priori or a posteriori various terms in the energy equation. Each model, of course, has a different interpretation for the physical description of the heating process. Probably the most important aspect in each theory is the assumption of boundary conditions placed on the variables. Each model undergoes changes as more experimental evidence is accumulated; therefore, the following discussion is simply a basic outline.

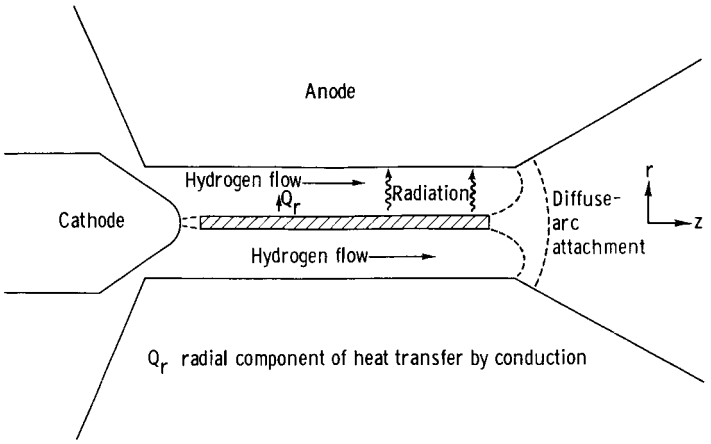

Figure 7. - Mechanisms of heat transfer in core-flow model.

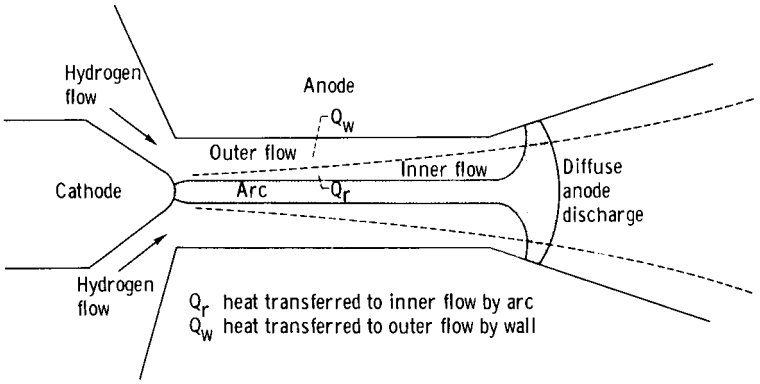

Figure 8. - Regions of flow and energy source for each in core-flow model.

Core-Flow Model

The positive column in the core-flow model is assumed to be a small extremely hot hydrogen "wire" (fig. 7, ref. 19). The basic energy equation, after the axial conduction and the convection terms are neglected, reduces to

$$\sigma(T)E^2 = P_{rad}(T) - \frac{1}{r}\frac{d}{dr}\left(r\frac{dS}{dr}\right)$$

The radiation term P_{rad}, a function of temperature at the given operating pressure, is often neglected when its contribution is small. Both parameters K and σ are calculated from analytically determined transport properties (ref. 18), which may involve considerable error because of the nature of the calculation. Note no axial, or z, dependent terms are included. Solutions to the preceding equations are obtained by applying boundary conditions on temperature (ref. 18). A number of solutions for various centerline temperatures are obtained from which an arc current and radius can be cal-

culated. The solution that gives the observed value for the arc current is taken as the physical case.

General features of the core-flow model are: A thin arc through which no mass flux passes (later this feature is modified) surrounded by an "inner flow" of very hot gas. This inner flow is in turn, surrounded by the "outer flow" of relatively cold gas (fig. 8, ref. 19). The purpose of the thin stagnate arc is to produce thermal energy and transport it to the inner surface of the inner flow, which can be thought of as a thermal boundary layer, the thickness of which increases in the axial direction. This gas then is heated directly by the arc and carries the main part of the energy. The relatively cool outer flow is not heated directly by the arc but by contact with the constrictor walls, which receive radiant heat from the arc and thermal conduction from other parts of the engine structure. Specification of the positive-column electric field, the pressure, and the boundary conditions then defines current, arc temperature distribution T(r), and arc radius. Of course, the temperature distribution of the gas is highly nonuniform causing a nonuniformity in fluid and chemical properties. The model can also be used for estimates of external body temperature distribution.

The assumption of negligible mass flux through the arc restricts the model too stringently. Calculations based on the solution to the energy equation as well as direct observation indicate a region of very high temperature near the center of the gas. Even though the mass flux may be small, the temperature is sufficiently high that the arc, especially the center, contains a substantial amount of enthalpy. This can be seen by comparing the axial enthalpy flow rate $\dot{H}_z$ with the total power dissipated in the arc $I \cdot V_{arc}$

$$\dot{H}_z = 2\pi \int_0^R r\rho u\left(h + \frac{1}{2}u^2\right)dr$$

where ρu is the local mass flux, h_o is the static enthalpy calculated on the basis of a stagnate arc (solution of the core-flow energy equation), u is the local speed of sound, r is the radial coordinate, and R is the radius of the arc. Estimates of $\dot{H}_z$ are as high as 15 kilowatts in a 30-kilowatt arc jet (ref. 21). The arc axial transport of energy can be accounted for without reconsidering and modifying the energy equation by assuming that the axial enthalpy flux is constant in the positive column. The source of this energy, then, is the transition region between the cathode surface and the fully developed column. The mechanism might be the acceleration of charged particles due to a large magnetic pumping force near the cathode surface (ref. 22) - the so-called cathode jet

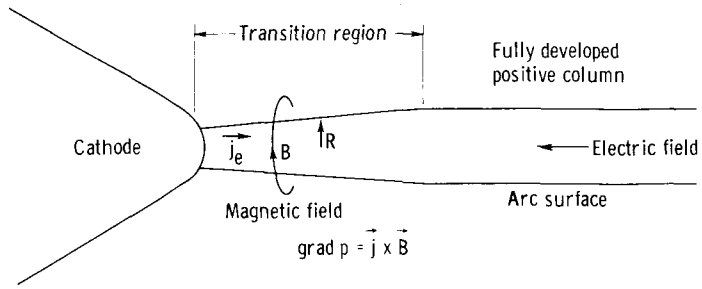

Figure 9. - Cathode transition region producing cathode jet. Axial pressure difference across transition region is responsible for cathode jet.

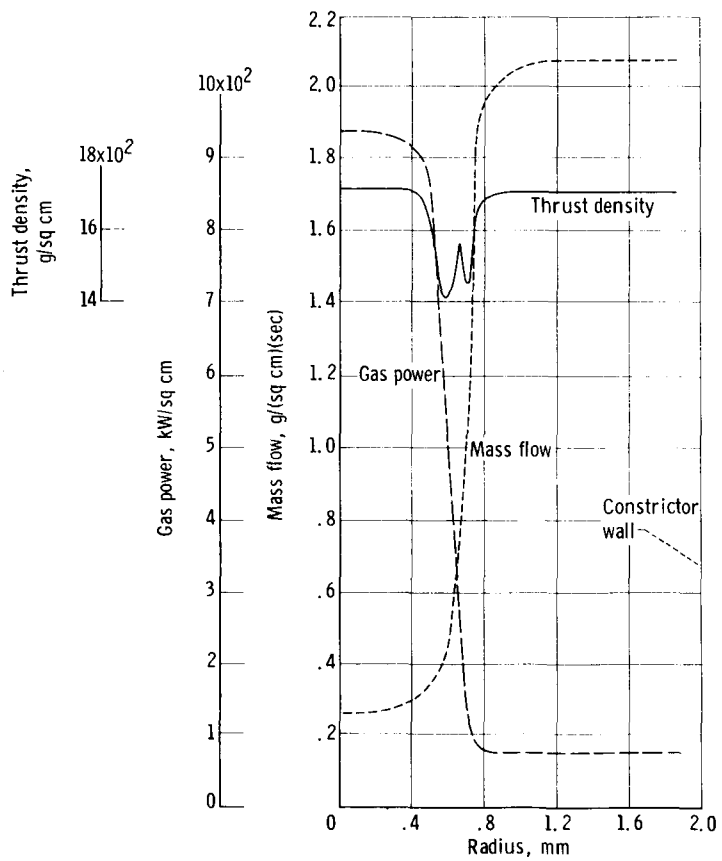

Figure 10. - Theoretical predictions of core-flow model for thrust density, gas-power density, and mass-flow-rate density. Input power, 18.4 kilowatts; hydrogen mass flow rate, 0.21 gram per second.

(fig. 9). The energy added in the transition region remains in the axial flow, which passes through the arc. Because there is no variation with respect to axial coordinate, the heat generated by the Joule heating processes passes into the inner flow, as explained previously. The main point to be made is that higher engine performance is predicted for the core-flow model than that predicted with the uniformly heated arc model because of an advantageous temperature and enthalpy profile.

It was shown that the performance (i.e., specific impulse and efficiency) of a device was dependent on the thermodynamic state of the propellant because of the frozen-flow phenomenon. In addition, it appears possible, under special conditions, to have improved performance because of the enthalpy distribution (ref. 23). Indeed, if temperature profiles similar to those of the core-flow model are used (ref. 19), the thrust is calculated to be about 10 percent less than the observed thrust, which incidentally is greater than the predicted value for the uniformly heated propellant model. If boundary-layer friction and other real gas effects are considered, the theoretical value should be even less. The variation of local thrust, power, and mass flux are shown in figure 10 (ref. 19) for the core-flow model at a power input of 18.4 kilowatts and a mass flow rate of hydrogen of 0.21 gram per second. Near the center

of the arc, the mass flow density is very small; however, the power density is large because of the high temperatures (above 30 000° K). The thrust density is shown to have a large value near the axis. Curves for higher power input have the same characteristic shape. In order to calculate an arc efficiency for this model, it is assumed that the inner flow (including the arc gas for this purpose) and the outer flow are independent concentric streams flowing in static-pressure equilibrium without mixing (ref. 19). Assignment of mass-flow-rate ratios and power ratios to the two flows, based on somewhat indirect evidence from measurements of the exhaust, allows calculation of an overall efficiency. It is significant that, for realistic mass-flow-rate and power ratios, an overall efficiency near that observed results; however, the arbitrary assignments leave something to be desired. More properly, if the efficiency were calculated, it should be taken from curves of the type shown in figure 10.

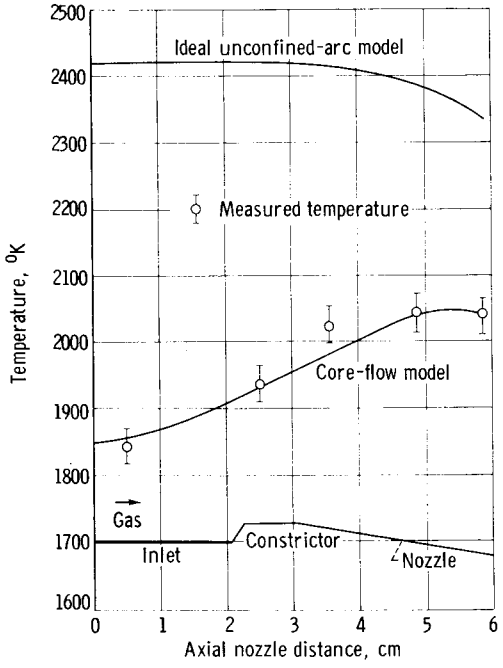

Figure 11. - Temperature variation with nozzle distance for core-flow and ideal unconfined-arc models for 30-kilowatt engine (ref. 24).

Other calculations made with the core-flow model (fig. 11, ref. 24) indicate the calculated axial temperature distribution along the inner engine wall. The observed values fit the core-flow model more closely than they fit the one-dimensional frozen-flow unconstricted-arc model. Although the calculated quantities sometimes differ from those observed, the predicted trends are quite often correct (refs. 18 and 19). Probably the basic drawback of the model is the inadequacy of explaining the axial enthalpy flux through the arc. The core-flow theory will continue to undergo change but is one of the better models for predicting arc-jet performance and characteristics.

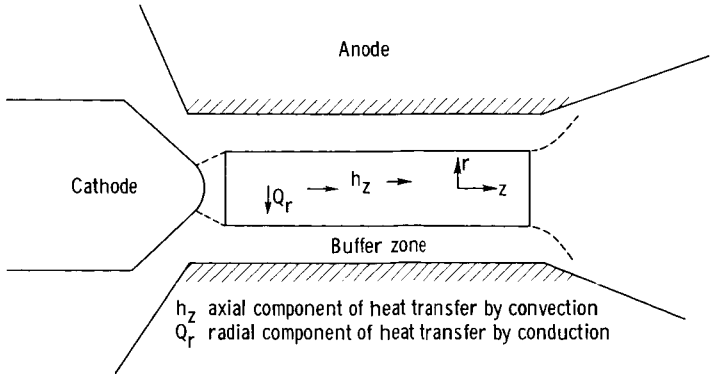

Figure 12. - Mechanisms of heat transfer in Stine-Watson theory.

Stine-Watson Model

The arc is assumed to fill a relatively large part of the constrictor in the Stine-Watson model (ref. 20). Essentially, all the gas passes through the arc (fig. 12). The energy equation after simplification takes the form

$$\rho v_z \frac{\partial h}{\partial z} = \sigma E^2 + \frac{\partial^2 S}{\partial r^2} + \frac{1}{r}\frac{\partial S}{\partial r} + \frac{\partial^2 S}{\partial z^2}$$

where ρv_z is assumed to be a constant. In this treatment the gas is air in thermodynamic equilibrium.

In contrast to the core-flow theory, the Stine-Watson model accounts for an axial convection term, the enthalpy gradient. The axial conduction term $\partial^2 S/\partial z^2$ is neglected after its solution indicated small contribution. The radial conduction term is considered to be an energy loss because of the small buffer zone between the arc surface and the constrictor wall. The contribution to the total-flow enthalpy of the buffer zone (some of the radial heat flux from the arc certainly remains in the buffer zone) can be calculated for many boundary conditions. The contribution seems negligible in every case. The energy equation is solved for the enthalpy $h(r, z)$ by assuming $h = (C_p/K)S$ and $\sigma = AS$, where $S = \int K\, dt$ (boundary condition $h = S = 0$ at $\sigma = 0$, C_p/K and A are constant at a given pressure, and σ is electrical conductivity in reciprocal ohms per foot (mho/ft). It is clearly an approximation to imagine that h and σ are linearly related to S. The equation is solved analytically by separation of the radial r and axial z variables (physically appropriate) to give

$$h(r, z) = C\left(\frac{C_p}{KA^{1/2}}\right)\left(\frac{I}{r_e}\right)\left(1 - e^{-11.5\frac{z}{z_0}}\right)^{1/2} J_0\left(2.4\frac{r}{r_e}\right)$$

where

h enthalpy, Btu/lb (boundary condition, $h = -3500$ at 0° R

C 9.43×10^{-3}

C_p specific heat at constant pressure, Btu/(lb)($^\circ$F)

K thermal conductivity, Btu/(ft)(^{o}F)(sec)

I arc current, A

r_e arc radius, ft

Z_0 $\rho u r_e^2 \frac{C_p}{K} = \dot{w} \frac{C_p}{\pi K}$, ft

$\dot{w}$ weight flow rate, lb/sec

J_0 Bessel function of first kind, zero order

ρ density, lb/cu ft

With the enthalpy as a function of radial and axial coordinates, many properties can be calculated; the local heat loss from the arc, the local voltage gradient, the radially averaged enthalpy at an axial position, the total heat loss from the surface of the arc, the total voltage drop over the length of the column, and the efficiency with which electric energy is delivered to the gas leaving the column. The most important trends for arc-jet application are that the radially averaged enthalpy leaving the column h_e is inversely proportional to the arc radius and proportional to the function

$$f(\ell) = \left(1 - e^{-11.5 \frac{\ell}{Z_0}}\right)^{1/2}$$

where ℓ is the column length. Also, the arc efficiency η_a, which is independent of current and arc radius, is given by

$$\eta_a = \frac{2f(\ell)}{\ln \frac{1 + f(\ell)}{1 - f(\ell)}}$$

As the constrictor length ℓ increases, $f(\ell)$ decreases and η_a decreases; hence, an efficient energy exchange takes place for a shorter arc (with the assumption that the arc is equal to the constrictor length). Laboratory devices have given some correlations between the Stine-Watson model and experiment (refs. 25 and 26). A striking agreement is given in figure 13 for the enthalpy parameter $h_e r/I$ plotted against length parameter Z/Z_0.

Originally the Stine-Watson model was conceived for arc wind-tunnel heaters in which, of course, no propulsive performance was derived. The model is being studied by others for arc-jet application (ref. 25), and some comparative propulsive data for

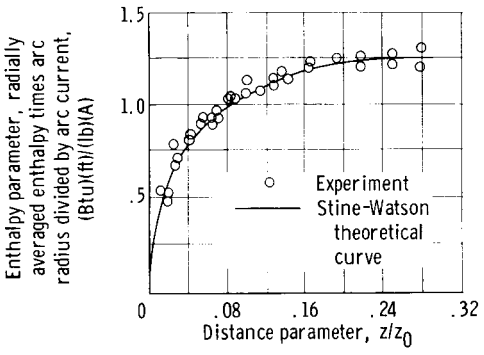

Figure 13. - Variation of enthalpy parameter with dimensionless distance parameter. Comparison of experiment with Stine-Watson model for nitrogen (ref. 26).

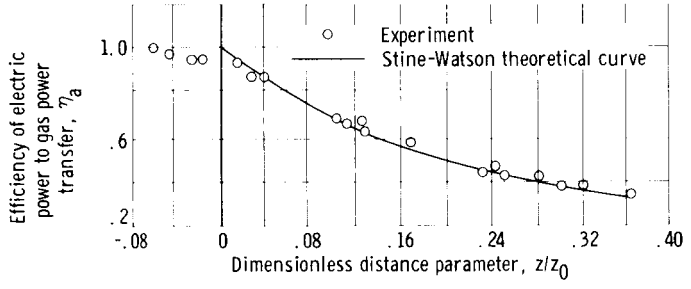

Figure 14. - Variation of arc efficiency with dimensionless distance parameter. Comparison of experiment with Stine-Watson model (ref. 25).

hydrogen are available. In this study, heat-transfer effects were correlated, and enthalpy ratios and arc efficiencies were plotted against an axial length parameter. Since the model does not apply strongly in the cathode region of the arc column, it was not surprising to find that the right trends were not predicted there. To determine the degree to which the trends are predicted, the experimental curves of the arc efficiency were fitted to the theoretical curves by a zero shift and two fitted constants, as shown in figure 14. Near the cathode, the Stine-Watson prediction falls below the experimental data. The fact that the heating process is much more efficient in the cathode transition region than that predicted by the Stine-Watson model indicates a power input not accounted for. Both the core-flow and the Stine-Watson models are admittedly not applicable near the cathode and neglect a region in which a pertinent heating mechanism takes place. In order to demonstrate applicability of the Stine-Watson theory to arc jets successfully, definite predictions of propulsion performance must be compared with experimental results. Alternately, success can be demonstrated by using the theory to design new arc jets of superior performance.

Both models of the arc-energy-transfer mechanisms can be fitted to certain experimental results by the appropriate choice of boundary conditions. The core-flow model is slightly more advanced in that it gives theoretical values for specific impulse and thrust even though they are consistently smaller than the observed values. Both models will continue to change as experimental effects are isolated and identified. Clearly, one region of interest is near the cathode. Substantial effects are noted here and subsequent influence on propulsion quantities are by no means insignificant; in some designs this region may be of major importance. Further work with the theory of arc operation may give some indication of the maximum propulsive performance that can be achieved with such a device and how to design it.

Summary of Arc-Jet Physics

For the purpose of analysis, arc-jet physics is divided into three regions: (1) the thermodynamics of propellants, (2) aerodynamics of the gas flow, and (3) arc-energy-transfer modes. In the first region, the frozen-flow phenomenon is introduced and some relations among pressure, enthalpy, temperature, specific impulse, and frozen-flow efficiency are graphically presented for various propellants. The frozen-flow efficiency relates the amount of energy available for thrust to the total energy in the gas. The description of the second region relies on the well-known fluid-flow equations for isotropic flow. Since the desired exit propellant speed is supersonic, the normal convergent-divergent nozzle is provided. Of importance is an empirically determined expansion efficiency, which relates the energy manifest in thrust to the energy available for thrust. Several models of arc operation have been proposed to describe the third region. Each of the uniform core-flow and Stine-Watson models assumes a certain mode of energy transfer, from which arc efficiency can be estimated or calculated. This efficiency relates the gas energy to the total input energy. Most of the current work in the physics of thermal arc jets is being done on the arc-energy-transfer modes.

ARC-JET ENGINE DEVELOPMENT

Engine development has proceeded along many paths in the past. At first, experimental methods were used; components were assembled and tested on the basis of a plenum-chamber-type heating process. Various modifications were tried in order to establish improvement trends. At certain points in engine development, theoretical guidance was needed; at other points experimental technique and material development were needed. It would be difficult to follow the arc-jet-engine development chronologically, but it can be presented in three sections: (1) design, (2) performance, and (3) outstanding problems. In each section, the relevant points of past and present are summarized, and each power level is discussed when general points cannot be drawn.

Design

Fundamentally, a thermal arc-jet design must provide two insulated conductors for the arc electrodes and a gas passage from inlet to exhaust. Because most current arc-jet designs are of the constricted-arc type, the discussion is based on a typical radiation-cooled design, as shown in figure 15. The cathode is a tungsten rod with a conical tip. The tungsten anode, which also serves as the nozzle, is placed slightly

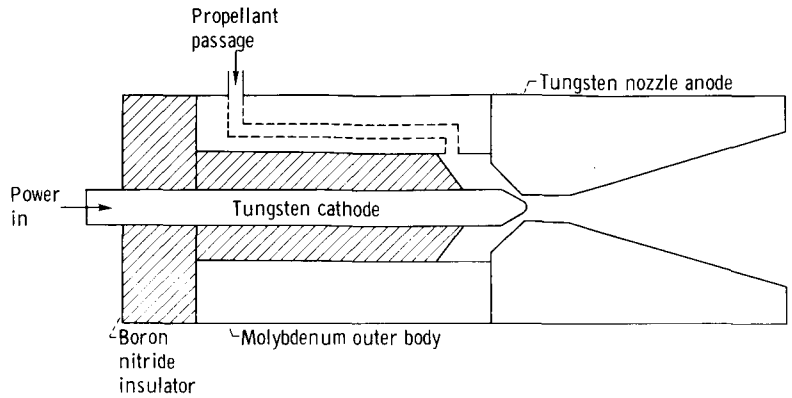

Figure 15. - General design for constricted-arc-type arc jet.

downstream of the cathode. The constrictor is the narrow horizontal portion of the nozzle. Surrounding the cathode is a boron nitride insulator. The outer body is made from molybdenum or tungsten. The back of the assembly is boron nitride, again for insulation purposes. The parts are sealed together by O- or C-rings and by close tolerances. The current is conducted into the cathode mounting from the power supply. The cathode is negative with respect to the anode. The propellant is led into the plenum by a passage through the upstream portion of the device and enters the arc cathode attachment region tangentially. Some regenerative cooling passages in the nozzle can also be designed as part of the gas inlet.

Motivations for certain aspects of the design are clear. For a given input power, the constrictor provides a larger arc than that possible in the unconstricted case; the former has a lower current than the latter. The cathode is the cone-tipped rod, and the anode is the massive nozzle because of the high heat load an anode must sustain; furthermore, the cone tip provides a high field region for thermionic emission of electrons. The flow enters the constrictor nearly tangentially in order to stabilize the discharge by creating a vortex that forces the cooler, heavier gas to the outer regions. It is questionable whether this vortex is really needed because data (refs. 25 and 27) show no significant change with vortex, at least in engines of 30 kilowatts of power and larger. In a smaller size engine (~1 to 3 kW), the vortex does have some effect, but until phenomena in this device are isolated, the role of the vortex cannot be correctly assessed. The nozzle provides more efficient conversion of random thermal energy to directed kinetic energy. It is thought that conical walls so nearly approximate the more properly contoured walls that the cost and complexity of machining the latter does not justify the effort.

Most of the engine failures have been the result of (1) nozzle cracks from thermal shocks, (2) arc anode attachment off the design point due to power fluctuations, or (3) leakage of critical engine joints. These effects can often be traced to deterioration by heat loads; therefore, the basic design must be considered from a heat-transfer aspect.

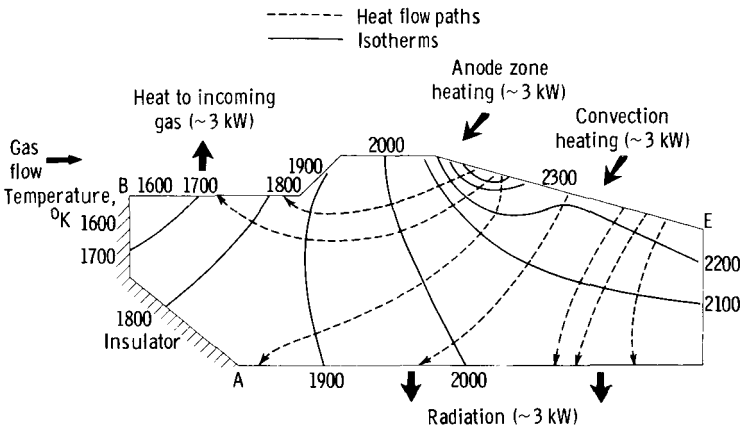

Figure 16. - Engine isotherms and heat flow paths for 30-kilowatt arc-jet engine.

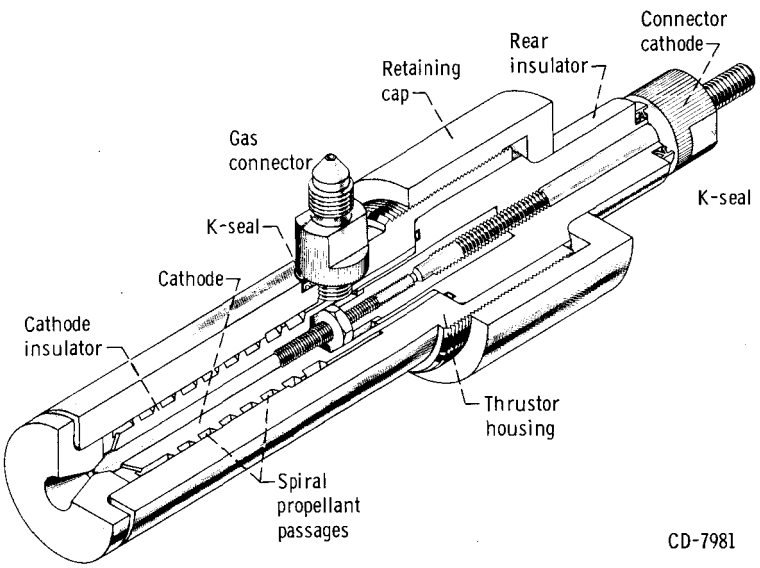

Figure 17. - Two-kilowatt direct-current arc jet (designed for NASA by Giannini Scientific Corporation).

This is largely a matter of experience and the specific design, but a few general rules can be set down. It was observed that the hottest part of an engine is the downstream end of the nozzle (refs. 24 and 28). To provide sufficient cooling by radiation, adequate surface area must be provided. Interfaces at high heat flux regions can cause detrimental hot spots. For this reason, the joint of the anode and the outer body should be made as far upstream of the nozzle end and constrictor as possible. A typical heat flow of an anode section in the steady state is shown in figure 16 (ref. 29). This was obtained by an assignment of local heat loads in the arc-nozzle flow passage and an experimental determination of outer surface temperatures by spectrographic and thermocouple means. Although details of heat loading differ for different designs and power levels, the trends are considered to be general for any size engine of the direct-current (d-c) type.

Specific engine designs of conventional arc jets will illustrate the various design

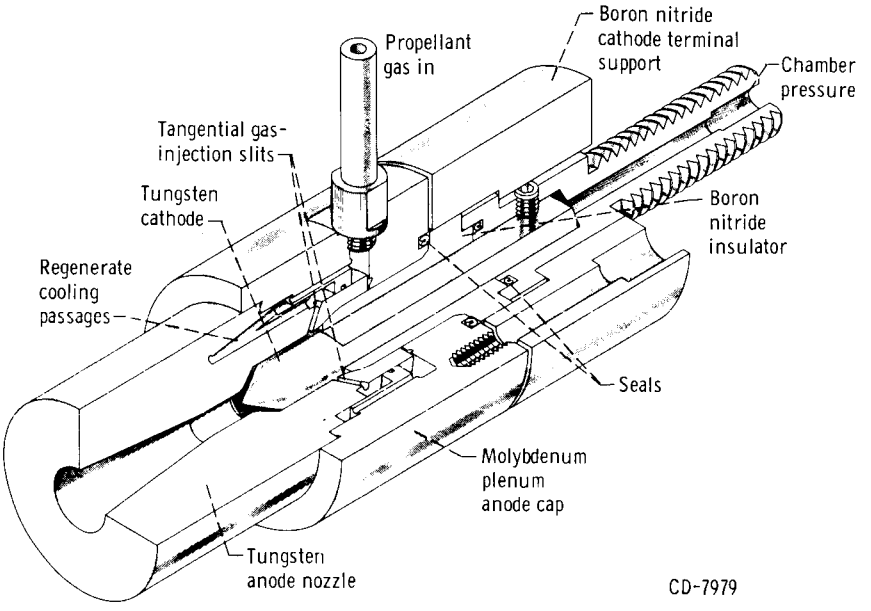

Figure 18. - Schematic diagram of 30-kilowatt direct-current radiation-cooled arc-jet engine (designed for NASA by Avco Corporation).

features. Figure 17 shows a 2-kilowatt engine design (ref. 30), which is typical of low-power arc-jet thrustors. The relatively large outside diameter of about 1.3 inches and the nozzle length of about 4 inches provide a large surface area to radiate excess heat. Regenerative cooling by the propellant is provided by the spiral inlet passage surrounding the cathode insulator. Characteristics of all engines of the low-power level are the small throat and nozzle dimensions. Although not easily discernible in the figure, the engine has a constrictor with a length to diameter ratio of 1 at the throat. A 30-kilowatt d-c design (fig. 18, ref. 19) has a relatively large nozzle area (~2-in. o.d. and overall engine length of 5 in.). The regenerative cooling passages in this design are axial, which help to cool the braze joint at the outer body and nozzle; energy is thus recovered that would normally be a heat loss. The 30-kilowatt d-c design in figure 19 (ref. 31) has the mixing chamber in the throat section. An initial constrictor section provides efficient heating, while the mixing chamber provides flow uniformity. A rather intricate propellant inlet passage consists of spiral regenerative cooling passages that divide the propellant flow so that a small amount enters along the cathode, while the main part passes through the labyrinth.

A critical distinction between direct-current and alternating-current (a-c) arc thrustors is the effect of the arc oscillation on the performance. Because the thermal relaxation time is about 10^{-3} second, single-phase a-c arcs of frequency higher than 10^{3} cycles per second behave like d-c arcs, except for electrode heat loading. The deleterious anode fall region alternates between electrodes and thus overloads the rod (central) electrodes to cause serious erosion. A three-phase a-c engine differs from the typical single-phase design primarily in the electrode-constrictor region. The

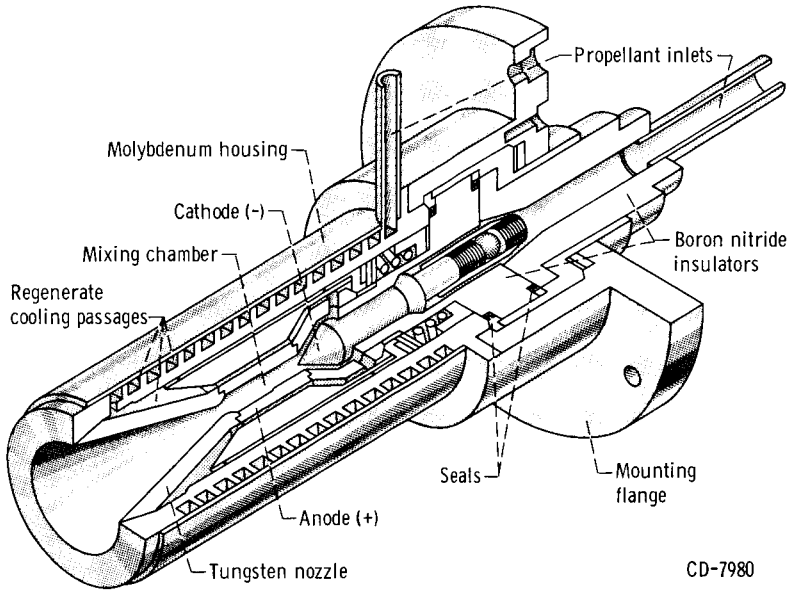

Figure 19. - Cutaway view of 30-kilowatt direct-current regeneratively cooled arc-jet thrustor (designed for U. S. Air Force by Giannini Scientific Corp.).

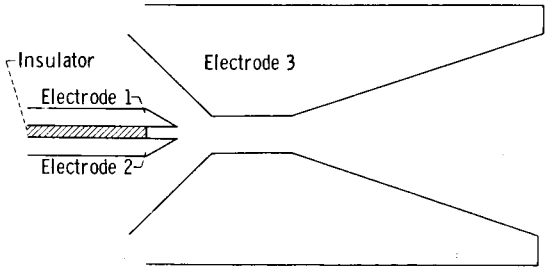

(a) Parallel center electrodes (ref. 32).

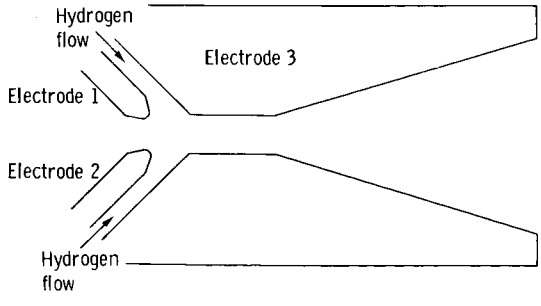

(b) Skewed center electrodes (ref. 18).

Figure 20. - Two designs of alternating-current arc jet.

phase of the potential is such that the arc strikes alternately between electrodes 1 and 3, 2 and 3, and the two rods 1 and 2 (fig. 20). The cathodes are separated by an insulator. The engine usually and more effectively operates in a delta connection formed by the three arcs. Overall heat transfer is similar to the d-c case, except for an increased input in the regions of the central electrodes. A three-phase a-c design (refs. 32 and 33), in which the two rod electrodes are asymmetrical with respect to the engine, is presented in figure 21. The constrictor and regenerative cooling passage are evident. A weld at the downstream nozzle end is not shown. Typically, the tangential flow inlet is near the rod tips.

Performance

Propulsion devices, no matter how theoretically feasible and perfect, must ultimately be judged on their performance, which for the

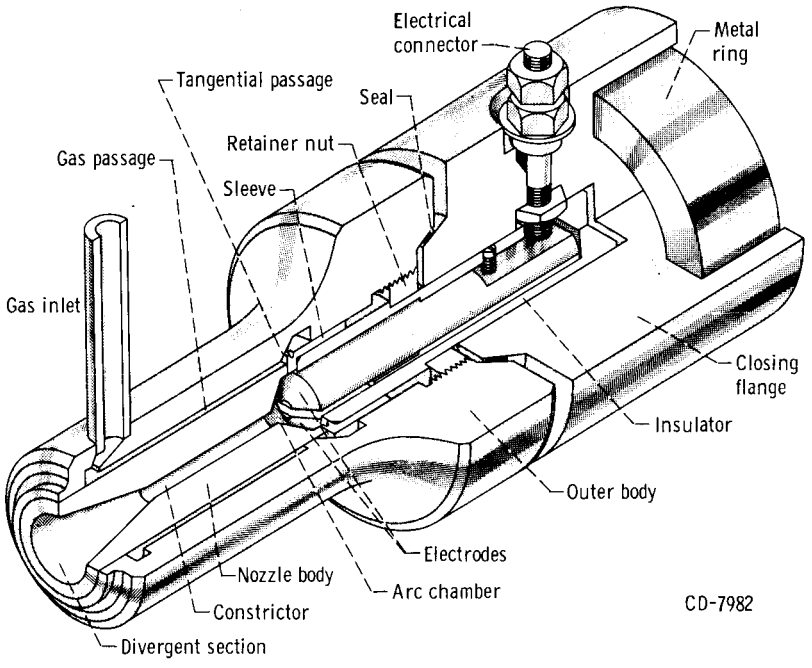

Figure 21. - Thirty-kilowatt three-phase alternating-current arc-jet thrustor (designed for NASA by General Electric Co.).

purposes of this report, shall mean specific impulse, overall efficiency (hereinafter efficiency shall mean overall efficiency), and lifetime. Only the last variable is directly observable; the first two variables must be calculated from experimental data as follows:

$$I_{sp} = \frac{T}{\dot{m}}$$

$$\eta_o = \frac{1}{2} \frac{T^2}{\dot{m}(I \cdot V + Pg)}$$

Effects influencing the observed engine-performance data are from many sources; tank back-pressure, which affects the thrust of the arc jet, is absent in space. The reported thrust, however, is the observed thrust (uncorrected for environmental conditions). Errors associated with the test instrumentation are usually not severe. The thrust stands are of the flexure or pendulum type with a positive displacement-force transducer. The accuracy of these stands (below about 25 g) in the very low thrust range becomes marginal. (It should be noted that the thrust level for the 1-kW arc jet is 5 to 7 g.) Therefore, extreme care must be used to obtain reliable data. Flow-rate measurement is accomplished with calibrated flowmeters and critical orifices. Electrical instrumentation has the typical measurement accuracy of about ±1/2 percent for the d-c measurements.

For the purpose of discussion, the thermal arc jets are classified according to power level with further subdivisions into direct and alternating current where applicable. The high-specific-impulse arc thrustor, in which self-induced electric and magnetic forces contribute significantly to the acceleration process, is considered separately. The power level may be designated as low (1 to 3 kW), medium (20 to 50 kW) and high (larger than 100 kW). More development effort has been expended for the low and medium power levels than for the high power level. Lifetime, mass flow rate, thrust, and specific values of overall efficiency and specific impulse vary with the power level. Because designs cannot be scaled from one power level to another, a specific design is necessary for each. Furthermore, analytical development is not generalized to all power levels. For these reasons, performance, interpretation, and problems vary with the engine design at different power levels. In general, recent designs for low and medium power are of the radiation-regeneration-cooled type; designs for high power are still in the experimental stage and are thus water-cooled. General data and operating envelopes are presented along with a description of other test conditions, but a discussion of specific problem areas will be postponed until a later section, ARC-JET SYSTEMS.

In the low power level, results are available for 1- and 2-kilowatt engines. A major difficulty at low powers is the stable operation of the thrustor. On the basis of one-dimensional frozen flow and desired performance, throat diameters for the 1-kilowatt engine are approximately 0.01 inch, which results in Reynolds numbers of about 200 (ref. 34). Severe heat loads were experienced with small engine sizes. Tests begun at certain thrust, specific impulse, and efficiency levels remained constant for a short time then began to decay. Operation of the engine was unstable as evidenced by large voltage and exhaust lumination fluctuations and erosion sparks.

In one effort to reduce electrode heat loading and to study the propulsive properties of other gases, many propellants were examined (table I, ref. 26) with negative results. The longest life test on a 1-kilowatt engine utilizing hydrogen for a propellant was 25 hours (ref. 34); the average performance over the first 12 hours was a specific impulse of about 1100 seconds and an overall efficiency of 35 percent. Performance decayed to a specific impulse of about 850 seconds and an overall efficiency of 20 percent at the end of the run. The test was terminated because of electrode erosion.

Many factors affect performance of the 1-kilowatt arc jet. The vortex motion, or swirl, of the inlet gas seems to have a pronounced effect on lifetime. For this size the centrifugal force (larger on the cooler heavier gases) keeps the anode throat cooler and lessens erosion. The electrode gas (arc length) has an effect on the 1-kilowatt device, as well as arc jets at all power levels. The gap (at a fixed gas pressure) determines the arc characteristic (voltage-current relation). It has been shown experimentally and theoretically that the performance is very much dependent on the current and voltage, which are, in turn, dependent on the gap and gas pressure. The shape of the cathode

tip, from conical tip to flat end, affects both the starting and steady-state operation. It is believed that a flat end does not provide an axial position of high field intensity in which to stabilize the arc. The causes of the dependence on these parameters are not known sufficiently to alleviate the problem.

The 2-kilowatt arc jet (ref. 30) was obtained by scaling from a 1-kilowatt design. The scaling was based on geometry, with separate consideration being given to the boundary layer. Primary parameters considered in this program were the throat (constrictor) diameter, axial electrode spacing, and propellant inlet configuration (fig. 22). The constrictor length to diameter parameter ℓ/d was kept between 1.5 and 1. The diameter d was varied between 0.015 and 0.035 inch with 0.005-inch intervals, and the axial spacing x ranged from 0.006 to 0.038 inch. For a given specific impulse, larger throat sizes were recognized as the best from lifetime aspects. Variations in axial electrode distance for a constant throat size indicated an optimum length of 0.026 inch (fig. 23). With a redesigned gas-injection pattern and a larger outer anode diameter (design similar to that in fig. 17, p. 21), an endurance run was performed with the 0.035-inch throat and the 0.026-inch axial-gap configuration. Nominal performance was as follows:

Thrust, lb	0.03
Specific impulse, sec	935
Efficiency, percent	30
Current, A	20
Volts, V	100
Test time, hr	150
Power, kW	2

Although the data indicate a formidable problem, it is by no means certain that low-power arcs are incompatible with high efficiencies required for a space-worthy propulsion device. To arrive at a definite conclusion for the feasibility of low-power arc-jet propulsion, especially at the 1-kilowatt power level, a program of systematic variation of parameters would have to be undertaken with a detailed knowledge of arc-energy-transfer mechanisms and operating conditions.

At the medium-power level (20 to 50 kW), the initial consideration of the arc-jet development was the effect on engine performance of structure cooling and flow nonuniformity. The arc-jet cooling system must radiate the heat transferred from the "hot" propellant to the "cold" engine structure. Obviously, any energy leaving the arc-jet system is lost for propulsion, as is shown in figures 24 and 25 (ref. 24) for water- and radiation-cooled designs. Water-cooling extracts more heat from the arc jet, resulting in lowered performance than radiation cooling. Most recent arc jets use a regenerative,

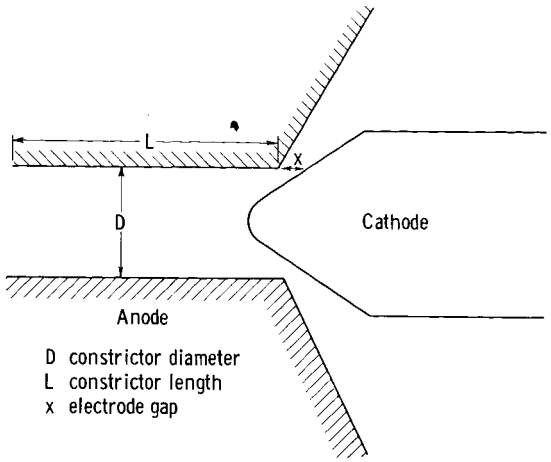

Figure 22. - Cathode-constrictor region showing important length parameters.

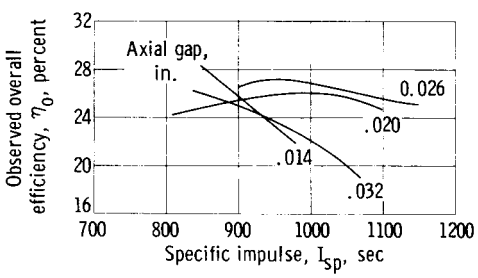

Figure 23. - Observed overall efficiency as function of specific impulse with axial gap as parameter. Power, 2 kilowatts; constrictor diameter, 0.035 inch.

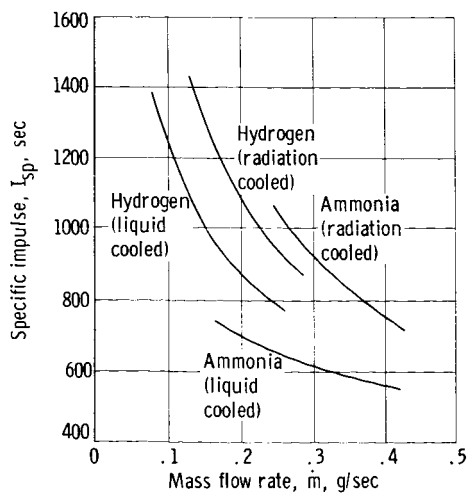

Figure 24. - Experimental curves of specific impulse as function of mass flow rate for water-cooled and radiation-cooled engines. Power, 30 kilowatts.

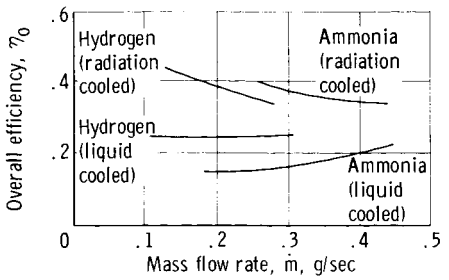

Figure 25. - Experimental curves of efficiency as function of mass flow rate for water-cooled and radiation-cooled engines. Power, 30 kilowatts.

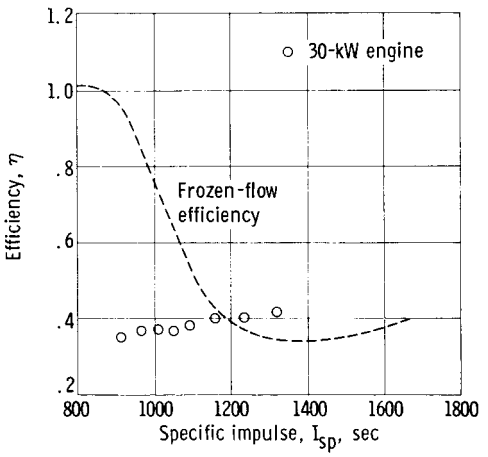

Figure 26. - Engine efficiency as function of specific impulse for hydrogen at 1 atmosphere.

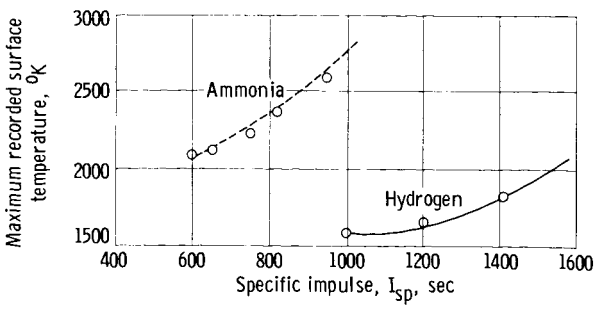

Figure 27. - Maximum surface temperature for ammonia and hydrogen as function of specific impulse (ref. 24).

radiative cooling scheme for the most efficient use of thermal energy. Flow nonuniformities in medium-power engines are expected as a result of the constricted-arc design. The curve for theoretical frozen-flow efficiency as a function of specific impulse for hydrogen at 1 atmosphere is compared with experimental points (fig. 26). Because the trend of the data points is different from the theoretical curve, the flow must not conform to the assumption of uniform one-dimensional frozen flow used in the calculation of the curve.

Verifications of other trends predicted by the preceding propellant considerations were also made in the early 30-kilowatt-engine development program. Hydrogen is an attractive propellant because of its high-specific-impulse and efficiency characteristics (figs. 24 and 25) and relatively low operating temperatures (fig. 27). Early data on the 30-kilowatt d-c arc jet from reference 24 are as follows:

Specific impulse, sec	1000
Efficiency (corrected for vacuum conditions), percent	42
Thrust, g	250
Test time, hr	50

The electrode erosion rate was of the order of 2×10^{-6} gram per second for both the anode and the cathode. For ammonia, the results are as follows:

Specific impulse, sec	720
Efficiency, percent	35
Thrust, g	300
Test time, hr	27

The major goals of later programs were to increase lifetime and specific impulse.

Present day designs for performance level and lifetime make the 30-kilowatt d-c thrustor a usable device. A design employing regenerative cooling, as shown in figure 18 (the propellant gas is used to cool critical regions of the thrustor preceding injection into the constrictor), has allowed runs as long as 30 days (refs. 19 and 35). Operating conditions for this thrustor with hydrogen as the propellant are:

Test time (30 days), τ, hr	723
Propellant flow rate, g/sec	0.25
Voltage, V	200
Current, A	150
Thrust, g	250
Specific impulse, sec	1010

Efficiency (uncorrected), percent	40.7
Electrode mass-loss rates, g/sec	
Cathode loss	2.56×10^{-7}
Anode loss	0.84×10^{-7}
Total loss	3.4×10^{-7}

The test was terminated voluntarily. On disassembly, the thrustor had a slightly sand-blasted effect downstream of the throat and a crater-like cavity in the cathode tip; however, no change in engine dimensions was detected. It is likely that the engine could have run for much longer. The reported electrode mass-loss rate is not considered severe. There are strong indications from short-duration tests that the major portion of the electrode erosion takes place during the first hours of a test. Along with demonstration of long life, high specific impulse has been achieved (table II, refs. 36, 37, and 45). A 250-hour test run, voluntarily terminated, with 1300 seconds specific impulse indicates that higher performance from conventional arc jets can reasonably be expected. Further improved specific impulse has been demonstrated by a 46-hour test at a specific impulse of 1500 seconds, a mass flow rate of 0.12 gram per second, a thrust of 180 grams, and an efficiency of 44 percent (ref. 45). Present day performance with ammonia is as follows (ref. 19):

Test time, hr	50
Mass flow rate, g/sec	0.25
Voltage, V	106
Current, A	283
Thrust, g	245
Specific impulse, sec	978
Efficiency, percent	38

This design is different from that for hydrogen because the higher temperature operation of ammonia requires a larger outside nozzle diameter to radiate excess heat, the thermodynamic properties of ammonia require a larger throat, and the electrical properties require a longer electrode gap than hydrogen at the same performance level. Table III (ref. 38) shows a typical operating envelope for a hydrogen designed arc jet and an ammonia designed arc jet.

The design that uses the mixing chamber concept (fig. 19) of a 30-kilowatt d-c engine has demonstrated long life at good performance levels; peak performance was (ref. 31):

Power, kW	30.3
Thrust, g	338
Specific impulse (vacuum), sec	1010
Arc chamber pressure, mm Hg	1105
Efficiency, percent	54
Arc voltage, V	261
Arc current, A	116
Test time, hr	500

The test was continuous over the 500-hour length with a voluntary termination. The quoted specific impulse has been corrected for vacuum (zero ambient pressure) conditions; the 54-percent efficiency is the highest attained at the 1000-second specific-impulse level.

Because the operation of this engine is believed to approximate the uniformly heated propellant model closely, it is likely that experimental performance is nearly that predicted by the frozen-flow analysis and is unlikely that the efficiencies at higher specific impulse will remain as high as 55 percent. Above an impulse of 1200 seconds, it is unlikely that the performance and life will be superior to that of the constricted-arc designs.

Concurrent with the development of the d-c arc jet was the development of an arc jet operating from an alternating-current source. Alternating current designs were originally thought to alleviate two apparent difficulties in d-c designs, that of electrode heat loads and thrustor compatibility with the power supply. Because the electrodes reverse polarity, it was thought that the heat loads would be less than in the d-c unconstricted-arc-jet design. Because the space power supply would most likely have a three-phase a-c output, direct connection to the thrustor might reduce power-conditioning weight. Present developments in both d-c engine design and power conditioning have made these two a-c advantages marginal. Because comparatively little work has been done on a-c arc jets, there may still be some advantages in the dynamics of an a-c arc-gas system. At any rate, it must be said that the stage of development of the medium power a-c arc jet is not as advanced as the d-c counterpart.

Reported peak performance of the three-phase a-c arc jet is similar to that of the d-c arc jet except for shorter lifetime and limited upper impulse range. Table IV (ref. 32) represents some typical performance figures. At 30 kilowatts, the specific impulse was about 1050 seconds, and the efficiency was 40 percent. Lifetime data available are for an engine of more recent design than the one represented in table IV. For 250 hours, the a-c engine was run at the following conditions (ref. 32):

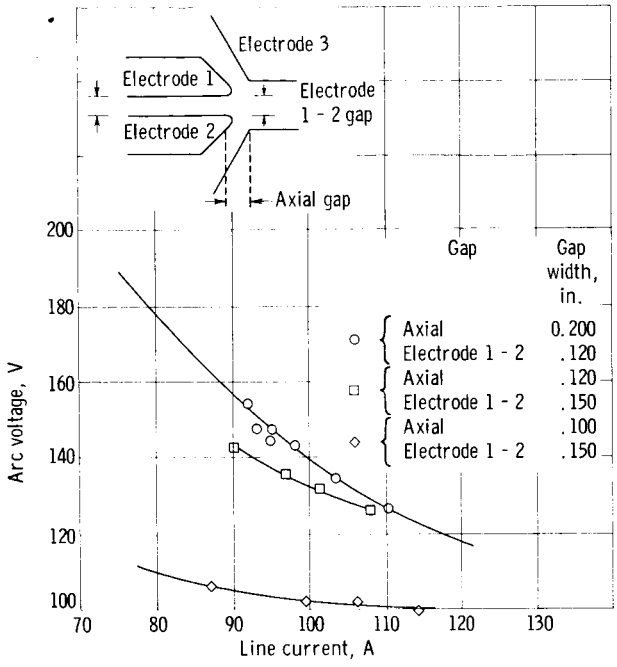

Figure 28. - Alternating-current engine arc characteristic at different electrode and axial gaps.

Power, kW	30
Thrust, lb	0.511
Specific impulse, sec	1022
Efficiency, percent	38
Mass flow rate, lb/sec	3.5×10^{-4}
Combined electrode ablation rate, g/sec	1.33×10^{-5}

Because of instrumentation failure, the preceding level of performance was not verified throughout the test. The test did prove, however, that the electrode-erosion problem in the a-c engine may permit reasonable engine operation for at least 250 hours.

In general, the three-phase a-c engine performance depends on the same parameters as the d-c engine, that is, gas swirl, axial gap between the electrodes, constrictor length, electrode material, gas flow rate, temperature, and pressure. In addition, the a-c arc characteristic and subsequent performance depend on frequency and central electrode gap (fig. 28). It has been established in both the d-c and a-c arc jets that there is substantial erosion at startup. Low-frequency arcs erode the electrodes more rapidly than high-frequency arcs. Because the thermal relaxation time for such an arc plasma is approximately 10^{-3} second, it is reasonably accurate to assume that frequencies of less than about 1000 cycles per second will exhibit the rapid arc-electrode-erosion phenomenon.

High-power thrustor (larger than 100 kW) development is in the initial development stage. Although radiation-cooled designs have recently been built, all previous work has been performed with water-cooled engines. Data obtained from the latter type is very useful in determining general operating conditions, performance trends, and theoretical insight to the physics of the system. An exhaustive study of water-cooled arc plasma generators (with nitrogen) of the type used for propulsion indicated the approximate range of operating conditions to be expected in high-power arc jets (ref. 18):

Current, A	200 to 1750
Voltage, V	150 to 450
Power, kW	25 to 500
Nitrogen flow rate, lb/sec	15×10^{-3} to 35×10^{-3}
Pressure level, atm	1 to 7
Constrictor diameter, in.	1/4 to 1
Constrictor length, in.	1 to 6
Arc efficiencies, percent	50 to 90

$$\text{Arc efficiency} = \eta_a \equiv \frac{\text{Power in gas}}{\text{Power to electrodes}}$$

The study was based on a design employing characteristics of the core-flow model, but some of the trends are also observed in other types of designs and predicted by other models. Some conclusions are (1) that the gas enthalpy is a strong function of the arc length (decreasing arc length increases enthalpy); (2) that at pressures above 5 atmospheres, the anode attachment of the arc becomes stationary and the electrodes erode severely; (3) that an effort to increase enthalpy tends to increase arc radiation, shorten arc length, and decrease the voltage gradient, thereby tending to reduce the arc efficiency; (4) that for a given mass flow rate, the enthalpy increases with constrictor (arc) length and the efficiency decreases.

There is some available unclassified data on hydrogen in a high-power arc-jet-type design and also some performance data on a high-power arc jet. On the basis of experimental plots of data taken from segmented-constrictor arc jets designed to approach the characteristics of the Stine-Watson model operating from 100 to 200 kilowatts, Cann and Buhler (ref. 25), arrived at an expression for the maximum enthalpy attainable in hydrogen as a function of constrictor diameter d_o (nearly equal to arc diameter in these experiments) and the current I;

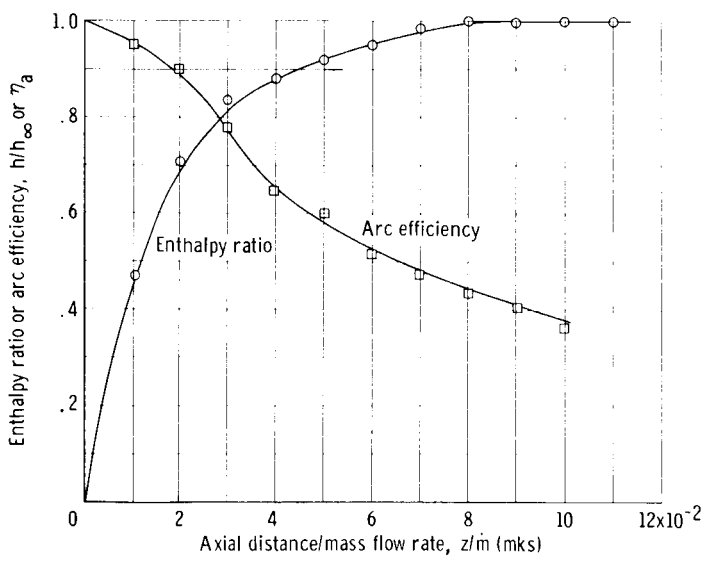

Figure 29. - Variation of arc efficiency and enthalpy ratio with axial length variable.

$$h_\infty \frac{d_o}{I} = 0.87\times10^4 \frac{(m)(J)}{(kg)(A)}$$

where h_∞ is the enthalpy at an infinite distance from the flow inlet. Use of this value in construction of figure 29 (ref. 25), where z is the axial coordinate measured from

cathode tip and $\dot{m}$ is the hydrogen mass flow rate, shows a qualitative trend mentioned previously; that is, the high enthalpy gas at a high arc efficiency needs only a short constrictor. Performance data are available on an engine that uses regenerative cooling of the cathode operating in the 200-kilowatt range with hydrogen (table V, ref. 37). These data indicate a high specific impulse (2080 sec) at a reasonable efficiency (37 percent) with several minutes of operation at each test point.

The performance of the "high-specific-impulse" arc thrustor is considerably different from that of thermal arc jets. At the high power levels, water cooling is generally used to protect the electrodes. Even with the energy loss associated with liquid cooling, performance is good. Representative results from one preliminary investigation (ref. 39) are given in table VI. Even higher values for the specific impulse and efficiency have been reported in reference 40 and are given in table VII. The two dominant variations in thermal-arc-jet operation are higher currents (for the same power level) and lower pressure. The tabulated enthalpy was obtained from the difference between the power input and power removed by the electrode cooling water, divided by the measured mass flow rate. A calorimetric measurement of the enthalpy in the exhausted propellant agreed with the calculated enthalpy to within a few percent. Stagnation temperatures associated with these values are of the order of 100 000° K. From the values of these performance figures and the poor correlation of thrust and plenum-chamber pressure (as opposed to a good correlation in the thermal arc jet), the conclusion is drawn that the nature of mechanism of the energy exchange is electromagnetic. The best performance of arc jets with hydrogen to date is given in table VIII.

Operating Problems

Most serious difficulties in conventional arc-jet propulsion devices are connected with the overheating of electrodes and other engine parts. Electrode overheating causes erosion of the material that results in shorter electrode life. Heating of engine parts, such as critical joints, may prevent engine integrity and hinder long-life performance. Historically, severe electrode heating was the first major problem encountered. Except at low power levels, solution of the heating problem elevates the materials problem to the fore.

In the medium and high-power arc jets, the electrode erosion is reduced to tolerable levels by two design characteristics. The anode, where heating is due to the large electric field near the surface, is designed to be the large downstream electrode; the cathode, which must provide electrons by thermionic emission according to electric current demands, is rod shaped and oriented so that the incoming propellant convectively cools it. The second design characteristic is the low-pressure region of the anode arc attach-

ment. By forcing the arc to attach slightly downstream of the throat (low supersonic velocity), where the pressure is much less than that of the plenum chamber, the arc forms a diffuse discharge, thereby distributing the anode energy flux over a larger electrode region.

Electrode erosion in the 2-kilowatt design is manifest on the downstream side of the throat, while in the 1-kilowatt size it is in the throat. The differences may only be due to the specific designs; it is likely that the cause or causes are the same. An inspection of the 2-kilowatt engine after its 150-hour test showed moderate erosion on the downstream side of the throat. The surface was irregular, exhibiting pits and masses of once molten tungsten. The primary cause is not certain. It is likely that both the heat flux associated with the flow thermodynamics and the heat flux associated with anode electron bombardment have nearly equal effects. In any case, erosion in this region did not seriously affect the performance of the engine over the test time. Longer test runs can probably be made without engine failure.

In existing 1-kilowatt thrustor designs, there is also a cathode-erosion effect. Rapid degradation of performance seems to occur when the diameter of the cathode tip approaches the throat diameter. This may be a spurious effect, but it does indicate, at least, some type of geometric electrode dependence.

Electrode erosion in the 30-kilowatt three-phase a-c design takes place on all the electrodes. Cathode erosion is present and seems to be a steady-state phenomenon with tungsten being lost at the rate of about 3×10^{-5} gram per second. Its effect is to flatten the half conical cathodes. Thus, the combined erosion effect is to lengthen the arc, sometimes to the point of blowout, as well as change the basic operating conditions.

Effective solution of the erosion problem in the 30-kilowatt d-c types by the low-pressure anode discharge has elevated to the fore problems in materials and fabrication techniques. As seen before, there are moderately high heat fluxes that an engine structure must conduct away without damage to critical regions, such as joints, welds, and boron nitride insulators. Thermomechanical effects like unequal expansion of dissimilar metals and thermal shock must be considered. Metallurgical problems arise in bonding engine parts together. Some studies are under way in analyzing material problems in arc-jet engines. There is one observed effect with the 30-kilowatt d-c engine that may influence long tests, and that is the craterlike formation in the tip of the cathode. The engine used in the 30-day run exhibited this formation, but observed constant performance over that period of time seemed to rule out any detrimental effect.

OTHER ARC-JET CONCEPTS

Concurrent with the development of thermal arc jets has been the search for new

ideas in arc-type propulsion. The target of most of the new ideas is the frozen-flow limitation. Schemes to lessen the frozen-flow loss include a bipropellant arc jet, a double-arc jet, and propellant recombination methods. Other ideas include thrust augmentation of an arc-jet exhaust by a crossed field (or $j \times B$) accelerator, radio-frequency heating of the propellant, and magnetic pumping of self-induced magnetic fields in the arc (the high-impulse arc thrustor). Before a discussion of a few of these ideas, some comments on the pertinent physical principles are in order.

The percent dissociation of a diatomic gas in equilibrium is a function of any two thermodynamic variables, such as the stagnation temperature and pressure or the stagnation enthalpy and pressure. The Mollier chart (fig. 2, p. 5), which is based on thermodynamic equilibrium, shows that a decrease in pressure at constant enthalpy increases the energy vested in dissociation of hydrogen, while an increase in pressure lowers the dissociative energy. With other losses remaining constant, efforts to use this high-pressure characteristic may be rewarded by an increase in usable enthalpy. If the heating process is appropriately divided into several steps, the maximum temperature-enthalpy restriction in the one heating step case can be avoided, as will be shown subsequently.

The dissociative energy in a diatomic gas can also be regained by inducing recombination of atoms by some appropriate technique. Recombination, of course, means that the gas is approaching its equilibrium state from its frozen condition. Atomic recombination can be accomplished by many atomic processes, the most dominant of which, for arc-jet expansion conditions, is the three-body collision among atoms. The residence time in the arc-jet nozzle, however, is still shorter than the three-body collision time, therefore little "natural" recombination is expected to take place (ref. 14). The recombination rate is dependent on the pressure and the degree of departure from equilibrium. Efforts have been made to enhance recombination by seeding the hydrogen propellant with a catalyst, which has a high collision cross section for hydrogen atoms (ref. 41), but results are inconclusive because the operating temperatures were lower than those that occur in the thermal arc jet. Although many efforts have been made to lessen the frozen-flow losses in the arc jet, these attempts have so far met with little success.

The bipropellant arc jet utilizes a gas with a low ionization potential to sustain the arc and a special nozzle contour to promote recombination. The concept envisions establishing the arc in a small amount of vaporized lithium and the injection of hydrogen so that complete mixing takes place ahead of the nozzle throat. The comparatively low temperature of the gas mixture would allow recombination if the expansion process is carried out properly - an initial rapid divergence in area (decrease in pressure) followed by a long slightly diverging region (fig. 30, ref. 42). The rapid divergence provides a large deviation from equilibrium to permit a tendency for fast recombination rates. The decrease in pressure must not be at so low a level that recombination is retarded. Thus,

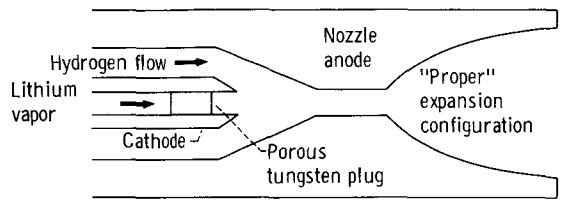

Figure 30. - Schematic design of bipropellant arc jet.

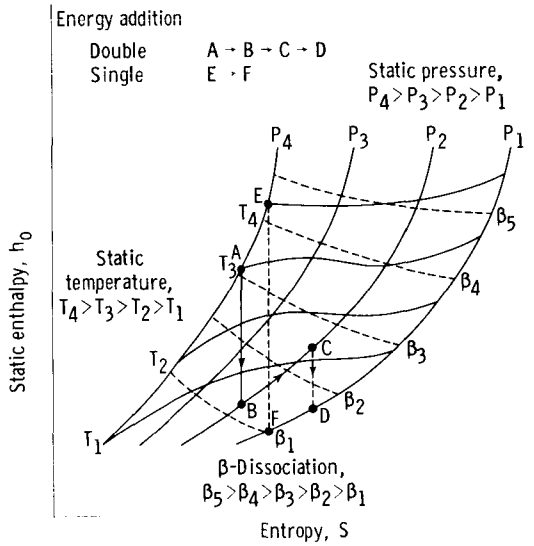

Figure 31. - Symbolic Mollier chart showing double and single energy additions.

the comparatively low temperature character of the mixture of lithium and hydrogen permits operation in a regime where an optimum temperature is attained, that is, the temperature of the gas that allows the proper expansion for recombination to occur. A more quantitative theoretical analysis of the bipropellant arc jet is available (ref. 42) along with a few experimental results, but verification of the proposed advantages over conventional arc-jet operation remains to be demonstrated.

The double-arc concept utilizes a two-step energy addition process in order to lessen the frozen-flow loss. For simplicity, all energy additions are assumed to be uniform. Qualitatively the theory proceeds as follows: The first energy addition takes place in the low subsonic region of the flow that is assumed to be in equilibrium. The state of the gas after the first heat addition then, is represented on a symbolic Mollier chart (fig. 31) as point A. An isentropic expansion (constant entropy) is carried out A → B that ends at a lower temperature and pressure. The second energy addition occurs at nearly constant static pressure B → C to a certain temperature T_0. The gas is then expanded, again, isentropically from state C to the ambient pressure. The dashed lines represent the frozen part of the expansion; hence, it cannot be correctly described on a Mollier chart, which is based on equilibrium. The flow is expected to become supersonic sometime during the second energy addition and therefore freeze shortly thereafter. But for reasons of simplicity the flow is assumed to be in equilibrium during the energy addition. The other dashed line E → F represents an isentropic expansion in the single-energy-addition case. Again, because the flow is frozen, the dashed line E → F represents the expansion only figuratively. The single point E is assumed to be an actual equilibrium state.

A theoretical comparison shows that, for a given plenum pressure and final stagnation enthalpy, the double energy addition by an appropriate division of power would have less dissociation (lower frozen-flow loss) than the single energy addition. In the latter case, the dissociation is defined by the given enthalpy and pressure. In the former case, part of the total enthalpy of the first energy addition is converted to gas velocity and a lower static enthalpy at point B. Since the dissociation is dependent on the static

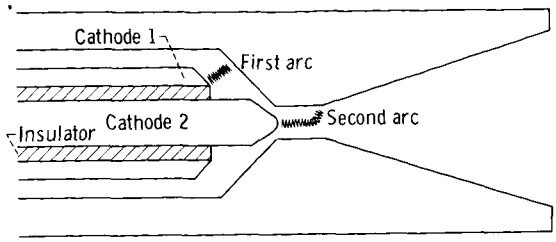

Figure 32. - Double-arc design of double-energy-addition process.

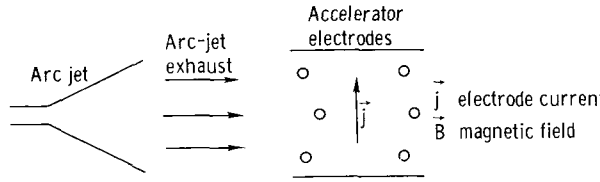

Figure 33. - Augmentation of basic arc jet with $\vec{j} \times \vec{B}$ accelerator. (Magnetic field perpendicular to page.)

enthalpy rather than on the stagnation enthalpy, the dissociation at B is less than at A (fig. 31). When the second energy addition takes place, the dissociation rises to the original value or higher but is still much less than the single-energy-addition case. Hence, for the final stagnation enthalpy at the same initial plenum pressure, the frozen-flow loss is lower in the double energy addition than in the single energy addition.

The double-arc configuration represents a practical way of accomplishing the double energy addition. Although no radiation-cooled engines of this type have yet been built, one limited study (ref. 43) was performed on an experimental design with two pairs of water-cooled electrodes (fig. 32). In this design, the first arc is believed to operate in the low subsonic region of the flow and is assumed to heat the propellant nearly uniformly. The second arc operates partially in the low supersonic region, therefore approximates conventional single-arc engines and is expected to heat the flow nonuniformly. The double-arc engine experienced difficulty in proper simultaneous operation of the arcs. The total electrical power could not be divided arbitrarily without causing serious instabilities; hence, it may not be possible to operate at the theoretical design point. To date, limited results indicate that the double-arc concept as a practical way of achieving the potential advantages of the double energy addition has met with little success. Furthermore, with the present arc technology it is unlikely that the double-arc concept will successfully develop into a propulsive system more effective than that of the conventional arc jet or some of its other derivatives.

Another practical way of accomplishing the double energy addition is by use of radio-frequency heating in conjunction with resistive or arc preheating. In various practical devices, utilizing radio-frequency energy in preheating the propellant greatly enhances performance, thereby approximating the two-step energy addition (ref. 44). Because some preliminary data indicate that the efficiency of energy transfer from input power to gas power in a radio-frequency heater (ref. 18) is low (about 10 percent for argon) it appears that the advantages of the double energy addition are not achieved by this concept either.

An additional concept that received some exploration was that of a $j \times B$ linear accelerator to augment a basic medium-power arc jet. Qualitatively, the theory of operation indicates that, if two parallel plane electrodes are placed downstream of the arc jet

(fig. 33) and a potential is applied to these electrodes, a current is established between them. If an external magnetic field is then applied parallel to the plane of the electrodes and perpendicular to the direction of the flow, the interaction of the accelerator electrode current j and the magnetic field B produces a force on the exhaust flow in the direction of the flow. Under ideal operating conditions, the result is to increase the specific impulse and efficiency. A limited program (ref. 45) that uses a basic 25-kilowatt arc jet provides some data and a few limited conclusions. The basic arc-jet performance was at a thrust of 124 grams, a specific impulse of 1030 seconds, and an efficiency of 24.6 percent. With the accelerator electrodes in position but not under power, the thrust decreased 16 grams indicating a drag force. Performance for hydrogen with power applied to the accelerator is shown in table IX.

The design point was at a total input power of about 60 kilowatts, approximately half of which is used by each thrustor device. The table shows that, at the design point, both the efficiency and the specific impulse have increased from the basic arc-jet performance. The data also show that the specific impulse increases above the basic arc jet for any total power; however, the efficiency lags until the design point is approached. Although accelerator-electrode erosion was severe, thus decreasing engine life, it can be concluded that, at the medium power level, the cross field accelerator increased the performance of the basic arc jet. The higher theoretical efficiencies are not attained because of energy losses due to electrode drag, Hall currents, ion slip, and charge depletion. The preceding program was concerned with the $j \times B$ augmentation of an arc jet. Other programs (refs. 46 and 47) have considered the $j \times B$ accelerator as a complete thrustor unit.

ARC-JET SYSTEMS

All electric-propulsion thrustors must be integrated into a flight system. Only when all system components are identified with definite performances and weights and are optimized with mission requirements should an electric-propulsion system be judged. Estimates, of course, can be obtained without ever putting together the entire package. Most of the work has been done at the 30-kilowatt power level with some data at the low power level. In general, component considerations fall under three categories: (1) power source, (2) power conditioning, and (3) fuel storage and feed system. The term power supply usually refers to the combination of the basic power source and the power-conditioning equipment. The status of these components will be outlined in the subsequent discussion.

Power Source

Space power sources of many power ranges have been under study and development since the space program was initiated. Many documents report the status and progress of these devices (ref. 48). It will suffice to summarize the powerplant capabilities with respect to the arc-jet operation.

The 1- to 3-kilowatt space-power sources take many forms: solar cells, batteries, fuel cells, and nuclear systems (SNAP-2). Currently, the most feasible are solar cells and batteries. A power supply study for a 1-kilowatt arc jet was made by Marshall Space Flight Center (ref. 49) in conjunction with a once proposed SERT flight. The basic power for this limited SERT voyage was to be supplied by zinc - silver oxide batteries. For sustained voyages, batteries become impractical, so a continuous-power-generation system must be employed. No definite system using the latter has been proposed, but consideration has been given to Sunflower and SNAP-2 (ref. 50), as well as solar cells for future space missions.

In the medium-power range, the turboelectric power systems generally referred to as the "SNAP 8" may someday be feasible. This power source, operating on a Rankine cycle, is expected to supply 30 kilowatts at 400 cycles per second, three-phase alternating current, 75 volts line to line, a 5-percent regulation, and a power factor of 0.9. These output characteristics are still flexible because of recent program changes. Because of the possible changes, a limited study of a power system was made (ref. 19) by assuming just a rotating shaft (12 000 rpm) supplied by the turbine of SNAP-8. Discussion of this power-conditioning equipment is deferred to a later section. Recent weight estimates of the SNAP-8 powerplant weight are 8000 pounds (see table X). Other power systems at the 30-kilowatt power level, such as solar collection, fuel cells, and thermionic conversion, have been proposed, but no experimental work has been done on their application to an arc-jet system.

In the megawatt range, some power-source concepts are similar to those at the 30-kilowatt power level. A SNAP-50 program at these power levels is under way. The feasibility of the turbogenerator power sources for arc-jet thrustors remains to be demonstrated.

Power Conditioning

The goal of matching the arc jet with the power system is one of establishing stable arc operation with a minimal power loss and weight penalty. Power-conditioning equipment must provide the arc jet with the proper electrical characteristics, such as voltage and current, by conditioning the output of the basic power source. Other requirements

on power conditioning may include starting circuits, overload protection, and changes in frequency. The general voltage-current relation of an arc - the arc characteristic - of the type used in propulsion is represented in figure 34. A constant voltage output of a power supply is represented by the horizontal line. Although a-c operation is not compatible with this type of power supply (the proper power supply can still be represented in the figure), the following discussion is, in general, applicable to any type.

For the arc to operate properly, certain conditions must exist between the arc characteristic and the power supply. Possible operating points are represented by the points of intersection of the arc characteristic and the power supply curves in figure 34. For the constant voltage supply, the intersection A represents an unstable operating point; that is, the arc operation will not be reestablished at that point if it is disturbed in any manner. To provide a stable operating point, the power supply must have a "drooping" characteristic. One possible way of achieving this is to provide an external resistive element in series with the arc, as shown in figure 34 by the negatively sloped straight line. The upper intersection B is still an unstable operating point, while C is a stable point. Because a drooping characteristic, providing the proper intersection, is all that is required of the power supply, it is possible to incorporate this into the design of the power supply. If the proper impedance is placed on the a-c side of a power supply in order to provide the drooping characteristic, the ballast resistor and the accompanying energy loss is dispensed with. Thus, the major function of power conditioning, to provide the system with a stable operating point, can be accomplished by only a slight energy loss.

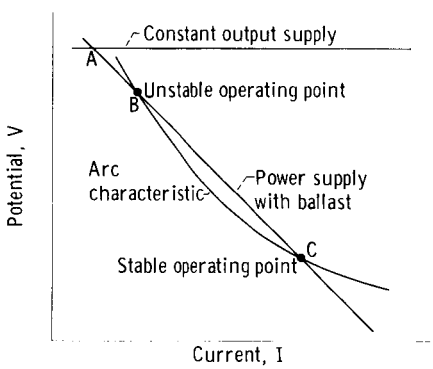

Figure 34. - Current-potential relation of arc, constant power supply, and power supply with ballast.

In the 1-kilowatt power level, the previously mentioned power supply (ref. 49) converts the direct cur-

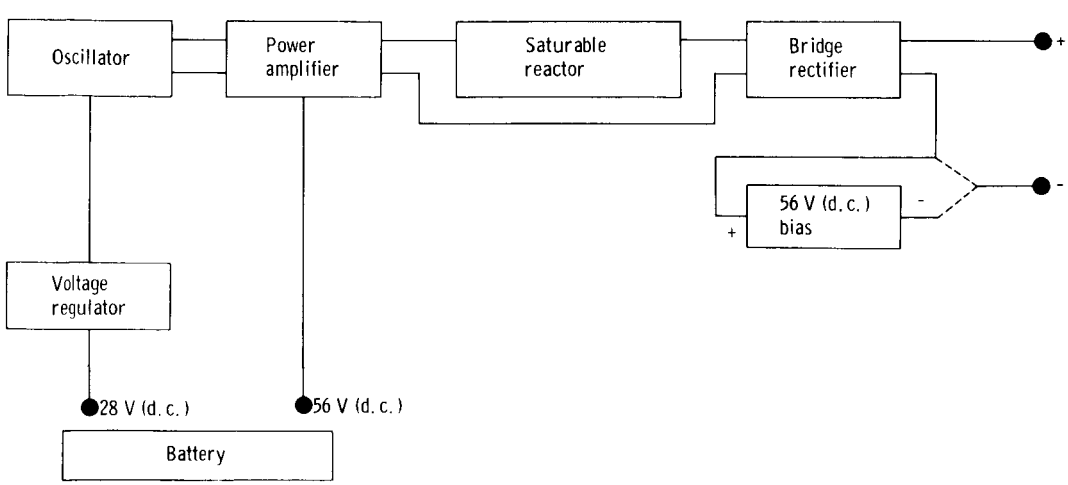

Figure 35. - Block diagram of 1-kilowatt arc-engine power supply.

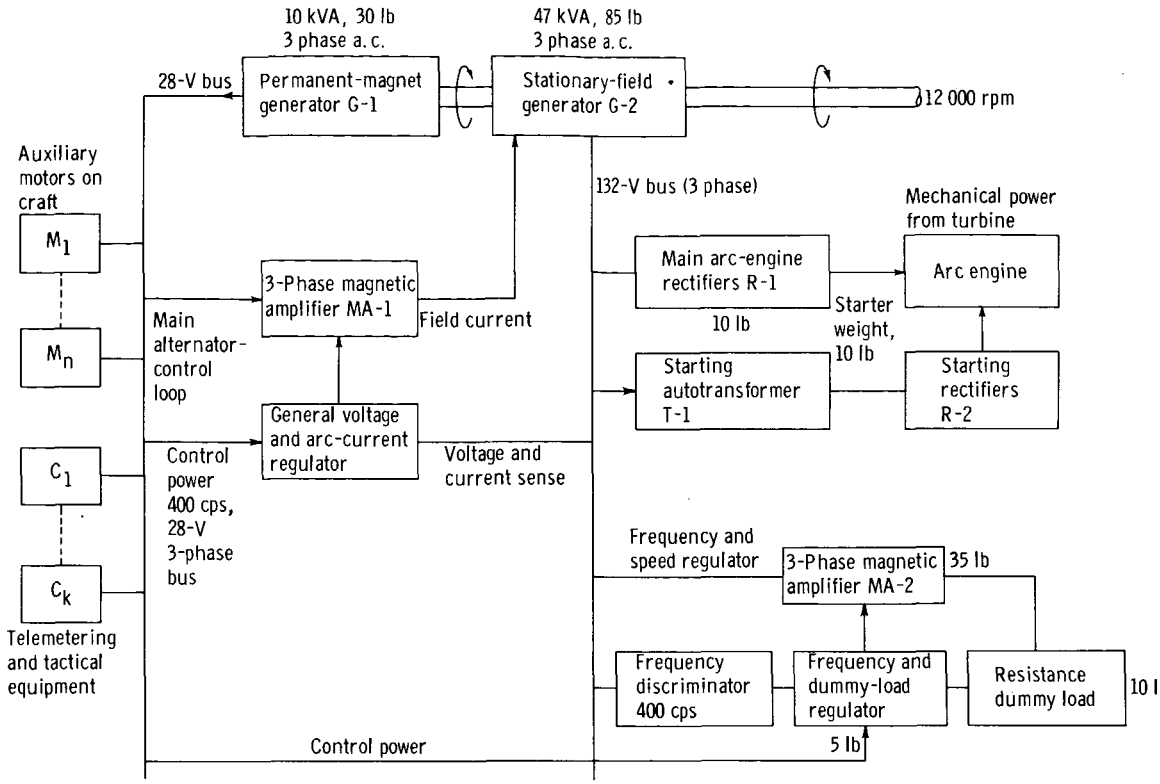

Figure 36. - Proposed SNAP-8 electrical system for arc engine and auxiliary load.

rent of the battery to a.c. then back to d.c. with the correct drooping characteristic. This d.c. to d.c. power supply (fig. 35) with a 56-volt battery provides a final output of 100 volts at 10 amperes with an energy-conversion efficiency of 90 percent. Incorporated in this power-supply design is an arc ignition circuit. The basic power-conditioning equipment (for the arc jet) and batteries weigh about 20 pounds (ref. 50). It should be emphasized that this study was for a once proposed SERT flight with only a short 25-minute engine operating time. Any other application may use many features of this power supply, but care should be taken in adopting the preceding values.

A power-conditioning system at the 30-kilowatt power level, which uses as input only the mechanical power of SNAP-8, has been suggested (ref. 19). Figure 36 shows the block diagram for such a system for the operation of an arc jet and auxiliary load. The mechanical power from a shaft rotating at 12 000 revolutions per minute is used in two generators, one a permanent-magnet rotor type, G-1, that is used to deliver a constant voltage to all motors and regulators. The other is a stationary-field type, G-2, whose output voltage is controlled by the field current that is ultimately controlled by the demands of the arc-jet engine. The current to the field generator is supplied by the magnetic amplifier, MA-1, which, in turn, is controlled by a regulator that senses the output from G-1 and arc-engine demands. Frequency and speed regulation of G-2 is controlled by a dummy load, a regulator, a frequency discriminator, and a magnetic ampli-

fier MA-2 assembly. The rectifiers, R-1, are a set of six silicon diodes arranged in a bridge circuit. These provide rectification for the steady-state operation of the 30-kilowatt arc jet operating at about 150 volts and 200 amperes. (Experimental results have shown such rectifiers to be at least 95 percent efficient with a power factor close to unity, ref. 24.) The rectifiers, R-2, and starting transformer, T-1, are the starting circuit for the engine. The three-phase transformer steps up the 132-volt supply to 215 volts (line to line) and limits the short-circuit current to 10 amperes. Rectification provides the 30-kilowatt arc jet with the necessary 300 volts starting potential.

The preceding system has many advantages. The generators have no rings or brushes, and because it is of inductive design there are no moving parts other than the rotating shaft. All components are conventional equipment, so no new technology is needed, thus the estimated system weight of 185 pounds is believed to be reasonably accurate. Although the preceding system has not yet been assembled in the complete form, there is little reason to believe there will be any difficulty. Power conditioning for high-power systems follows the trend of medium-power systems, although no definitive study has yet been made for arc-jet application.

Fuel Feed and Storage

The purpose of an arc-jet fuel-storage system is to store a sufficient amount of fuel (hydrogen or ammonia) needed to achieve the mission for which the arc jet is used. The storage of ammonia is relatively easily accomplished, as no new demands are put on present technology. On the other hand, hydrogen storage puts considerable demands on present technology in order to provide an efficient lightweight system. The high insulation and structural integrity at low-temperature requirements can only be accomplished with a given weight penalty. The relatively light weight and simplicity of the ammonia storage system results in a considerable advantage for ammonia. The choice between a hydrogen propulsion system (higher engine performance but a larger system weight) and an ammonia propulsion system (lower performance but lighter weight) rests with the requirements of a specific mission.

Several preliminary studies were initiated in order to identify specific storage problem areas and critical parameters, and to estimate system weights for both hydrogen and ammonia. Two mission profiles were considered. One was the attitude control of a satellite accomplished by a 1-kilowatt arc jet operating in a pulsed mode for 3 years. The other was an 85-day satellite raising (from 500-mile parking orbit to 22 000-mile synchronous orbit) by a 30-kilowatt arc jet propelling continuously.

The results of two studies (refs. 51 and 52) for the mission using the 30-kilowatt engine are summarized in the following discussion and in table XI. Cryogenic hydrogen

can be stored by two methods - subcritical and supercritical. The former is the storage in the liquid-vapor phase (below the critical temperature and pressure); the latter is storage in the gaseous phase at high pressure. High pressures, of course, require heavyweight structures. Very generally, then, subcritical storage has a weight advantage but difficulties in liquid-vapor separation and storage. The supercritical method has the advantage of single-phase storage and handling in a zero-gravity environment but difficulties in construction and system weight. The storage method chosen by each study was the subcritical one because of the lower tank weight.

The optimum configuration of the storage tank is determined from a consideration of structural strength, ease of applying effective insulation, and compatibility with other systems in the carrier vehicle body. The studies showed that subcritical storage of hydrogen in a cylindrical tank (with hemispherical ends) made from a 5-percent-aluminum 2.5-percent-tin 92.5-percent-titanium alloy best fills the storage-system requirements. For a total propellant weight of 3885 pounds, a total tank volume of 919 cubic feet is required for an assumed 5-percent ullage and a tank pressure of 45 pounds per square inch absolute. The tank dimensions are 16.2 feet long and 9.5 feet in outside diameter. Surrounding the tank is a layer of foam insulation with an apparent thermal conductivity of 0.30 (Btu)(in.)/(hr)(sq ft)($^{\circ}$R). Stapled to the foam is a layer of multifoil superinsulation (apparent conductivity, 2×10^{-4} (Btu)(in.)/(hr)(sq ft)($^{\circ}$R)). To mount the tank onto the vehicle structure, while providing adequate thermal insulation, nylon netting, straps, and glass-reinforced-plastic rings are employed. If a nuclear-electric power supply is used, adequate protection of the storage system from gamma radiation or heat leaks can be obtained without heavy shielding by placing the power supply and storage system at least 20 feet apart. The storage system weight, less the fuel, is 603 pounds and, including the flow controls, requires 1 kilowatt of power to operate.

The storage system for ammonia is also summarized in table XI and compared with the hydrogen system. Ammonia is stored subcritically in the liquid phase. The tank is made of the same titanium alloy as that used for the hydrogen system. A large, tolerable heat leak permits a toroidal shape. Such a shape simplifies packing problems. The storage-system weight, less the propellant, is 433 pounds.

The factor that makes the hydrogen system look superior to the ammonia system for the specified mission is the total weight of the propellant. Because of higher engine performance with hydrogen, only 3885 pounds of hydrogen are required to accomplish the mission, whereas 4740 pounds of ammonia are required. It still is not certain, however, that an actual hydrogen storage system of this size can be built according to the previous study. The critical items are insulation and insulation attachment. Because the cryogenic storage of hydrogen in a space environment is important to many other programs, studies are currently in progress under the Centaur Program (ref. 53).

The storage-system studies for attitude control with a 1-kilowatt engine (refs. 54

and 55) are summarized in the following discussion and in table XII. The method of hydrogen storage is subcritical. The amount of hydrogen needed for this 3-year period is 20 pounds. The tank configuration is a sphere 2.17 feet in outside diameter. The 1-kilowatt system uses the same titanium alloy as the 30-kilowatt system. The tank is covered by a load-bearing fiber-glass aluminum-foil insulation (1.43 in. thick) and a vacuum shell of twice the tank thickness (the same titanium alloy described previously, 5Al-2.5Sn-92.5Ti). Surrounding the shell in order are nonload-bearing aluminized Mylar layer insulation (apparent conductivity, 10^{-4} (Btu)(in.)/(hr)(sq ft)(^{o}R)), a hydrogen-vapor-cooled aluminum shield, and then more nonload-bearing insulation. Thin aluminum foil forms the outer covering. The support ring is made from the titanium alloy, 5Al-2.5Sn-92.5Ti. This proposed insulation system provides enough protection so that the boiloff produced by the uncontrolled heat leak satisfies the engine propellant requirements. This storage system, less the propellant, weighs 22.07 pounds. It should be emphasized, however, that the overall thermal conductivity used in the design may be optimistic. Less efficient insulators would increase the system weight. The proposed system has not been built, thus the design weight has not been confirmed. An alternate low-flow-rate system used external refrigeration. Use of refrigeration relieves the insulation requirement and the venting problem. If a Claude or Brayton cycle refrigeration scheme is considered, the weight of the system, less the propellant, is about 110 pounds, including a 50-pound penalty for additional power. Obviously, a long term mission (e.g., 3-year life) will be dependent on insulation until a lightweight refrigeration system can be developed.

The low-flow-rate system for ammonia is very similar, apart from total weight, to the high-flow-rate system. For the low-flow-rate system, ammonia is stored in liquid form in a spherical tank made of a titanium alloy. A gelling agent is used for the control of ammonia in a zero-gravity environment. The total ammonia propellant needed to accomplish the mission is 27.5 pounds. The storage-system weight, less the propellant, is only 7.12 pounds. Thus, the weight of the ammonia system including the propellant is 34.62 pounds. On the basis of total system weight and development capability within the existing state of the art, the use of ammonia is desirable.

Summary of Arc-Jet Thrustors and Systems

Research and development of the thermal arc jets have provided thrustors in the 1000- to 2000-second specific-impulse range. At low electrical input power, a 2-kilowatt thrustor has shown performance of a specific impulse of 935 seconds and an

efficiency of 30 percent for 150 hours of operation. At 30 kilowatts of power, engines have operated from 1000 to 1500 seconds specific impulse. Endurance tests have demonstrated that several designs have long life and good efficiency; 500 hours at 1000 seconds specific impulse and 55 percent efficiency; 120 hours at 1500 seconds specific impulse and 43 percent efficiency. At high power inputs, engines of 2120 seconds specific impulse and 35 percent efficiency have been developed, but no long-life tests have yet been attempted. Recently, experimental high-impulse arc thrustors operating in a nonthermal arc-jet mode have developed performance up to 10 000 seconds specific impulse and 46 percent efficiency. Preliminary studies of arc-jet systems have indicated the feasibility of component development. At low power levels, solar cells (batteries for limited flights) in conjunction with a low-weight power-conditioning system have been proposed. At 30 kilowatts, a nuclear-electric (SNAP-8) power source at weight estimates up to 8000 pounds and an independent power-conditioning system at 185 pounds has been proposed. At higher power (300 kW) SNAP-50, which is under limited development, has been suggested. Although propellant-storage systems have been studied for only two mission profiles, the results indicate the magnitude of the system weights.

MISSIONS FOR ARC-JET THRUSTOR

It has now been established that the arc-jet thrustor can operate at certain power levels with reasonable efficiency and endurance. The next question to be answered is "To what use can this engine be put for space missions in the foreseeable future?" Answers in the recent scientific literature range from the direct statement that "The arc jet is not interesting for space propulsion," (ref. 56) to the assertion that this thrustor is the best means of accomplishing a variety of missions in cislunar space (ref. 57). An attempt will be made to analyze three of the most often mentioned tasks for the arc-jet thrustor: (1) satellite "raising" from a given orbit to a higher one; (2) lunar ferry or transport, where a given vehicle is propelled from an Earth to a lunar orbit; and (3) attitude control or station keeping of an orbiting satellite.

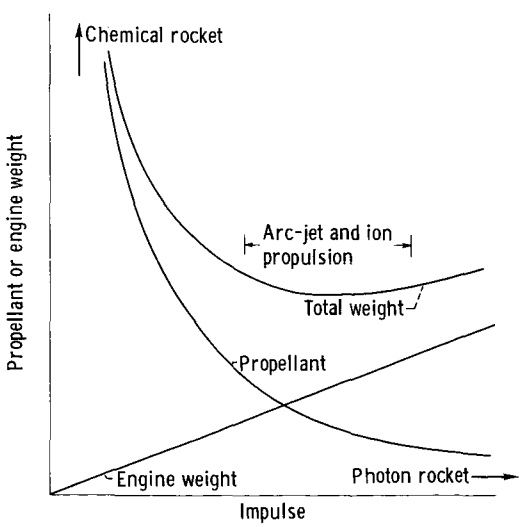

Figure 37. - Optimization of space propulsion systems.

The great importance attached to specific impulse, as indicated by published mission studies (refs. 1 and 5), is represented schematically in figure 37, which shows the variation of propellant

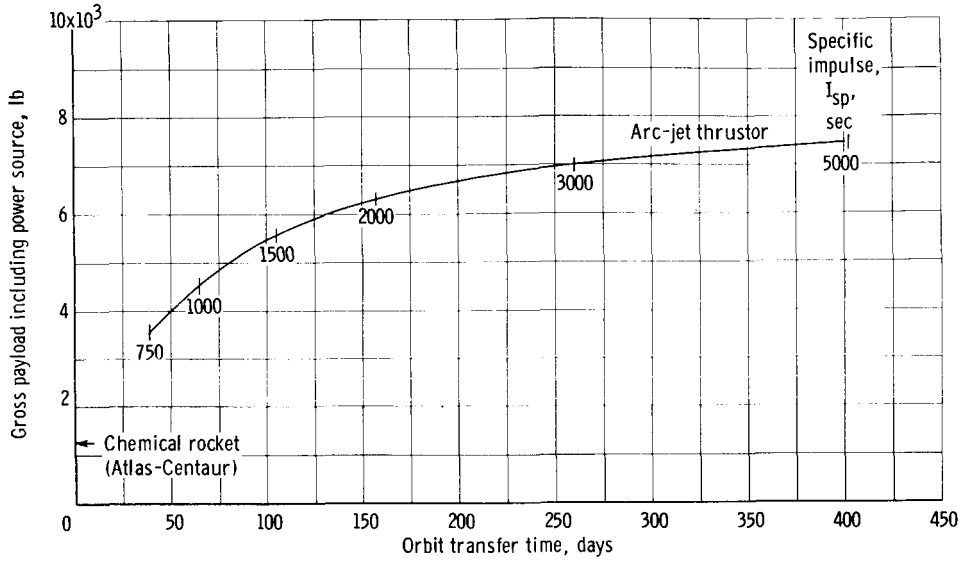

Figure 38. - Effect of specific impulse on gross payload for synchronous mission.

weight and engine powerplant weight as a function of specific impulse. Total propellant weight plus engine weight rises exponentially as impulse is reduced with the chemical rocket. At the opposite end of the impulse scale, the total weight starts to rise again because of the increasing importance of engine weight. The impulse range for the arc-jet and ion thrustors is seemingly a pleasant optimum in terms of total weight. On the basis of such results, the scientific community by and large has been most enthusiastic about the development of electric thrustors. In the subsequent mission studies, it will be demonstrated that there are additional factors that must be considered in the selection of a space-oriented propulsion system.

Satellite-Raising Mission

The most widely proposed mission for the arc-jet thrustor has been that of raising an orbiting satellite around Earth from a given altitude to a higher one, specifically, to the synchronous altitude of 22 300 miles. For this mission, many analysts have shown the arc-jet thrustor to have considerable advantage over the chemical rocket (refs. 1 and 58). A typical plot of gross payload including a 30-kilowatt electric powerplant is shown as a function of orbit transfer time for an arc-jet thrustor with a hypothetical impulse range between 750 and 5000 seconds (fig. 38). The 6000-pound payload available with the arc thrustor at an impulse of 1750 seconds (using an Atlas chemical booster rocket) is a large improvement over the 1200-pound payload with the all-chemical rocket propulsion.

If a 30-kilowatt electric-generating system weighing only 1500 pounds were available

(this is the weight that was once predicted for the SNAP-8 system), the 6000 pounds of gross payload weight provided by the arc jet would be sufficient for this mission. The 1200-pound weight available with the all-chemical system would not be sufficient for the mission. It was analyses such as these that made the case for development of the arc jet.

The actual weight of the SNAP-8 electric generating system, however, is now expected to be about 8000 pounds. Component weights for the early SNAP-8 conceptual design are compared with current component weight estimates in table X. Thus, with the electric-generating system actually available, the mission previously discussed cannot be accomplished with the Atlas-Centaur vehicle.

Nonetheless, it is still interesting to examine the mission-time factor, because it is an important but little considered parameter in the raising mission. The objective of the satellite at the synchronous altitude is often stated to be for communication purposes (refs. 1, 58, and 59). It is suggested in reference 58 that most of the 30 kilowatts of available electrical power from a SNAP-8 generator in a synchronous orbit could be used for television channels in the United States and South America. Presuming that this might be a worthy cause makes it interesting to examine the duration of this communication system. On the basis of a 10 000-hour operating life of the power generator, if 132 days or 3168 hours are used for the arc thrustor operating at 1750 seconds impulse to propel the system to the synchronous nonequatorial altitude (fig. 38), there is a remaining transmitting life of 6832 hours. Considering the very long life of a transoceanic communication cable and the general requirement of long service time where extremely high replacement costs are concerned, the assumption of using the electric power source as part of the payload is open to question.

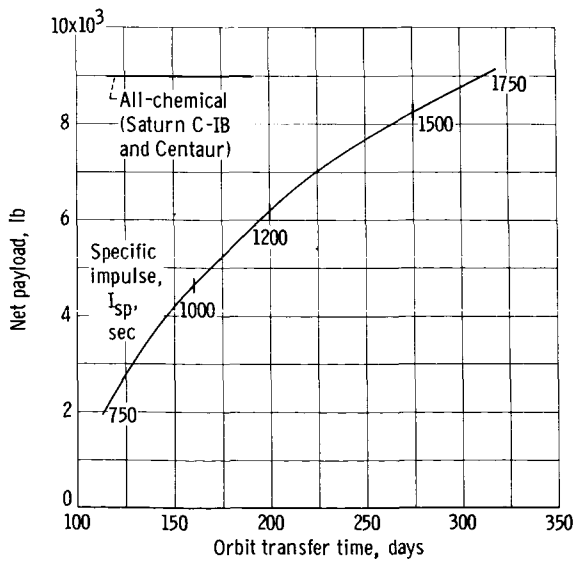

Figure 39. - Comparison of net payload available for synchronous mission using all-chemical and arc-jet thrustor propulsion. Power generation specific weight, 245 pounds per kilowatt.

It is evident then that to perform the satellite-raising mission (synchronous altitude) at all with the SNAP-8 electric powerplant will require a larger chemical booster than the Atlas-Centaur combination. For this reason, a similar satellite-raising study was made comparing the arc-jet thrustor with the Centaur upper stage and the Saturn IB as a first stage (calculations performed by R. J. Lubick of Lewis.) Net payload at the in-plane synchronous orbit is shown as a function of orbit transfer time for a range of impulse levels with an overall arc-thrustor efficiency of 50 percent (fig. 39). To equal the 9000-pound net payload available with the all-chemical

system, the arc-jet thrustor must operate at an impulse level of about 1750 seconds, with a resultant raising time of about 310 days. To calculate the curve presented in figure 39, the following assumptions were made:

(1) Initial gross weight of 26 000 pounds in a 300-mile circular orbit

(2) A 30-kilowatt arc-jet thrustor operating with an overall efficiency of 50 percent

(3) Vehicle characteristics

(a) A 30-kilowatt electric powerplant weight of 7350 pounds (It is assumed that the 8000-lb weight (table X) can ultimately be decreased.)

(b) Propellant tank weight equals 20 percent of hydrogen propellant weight

(c) Structure weight is 5 percent of initial gross weight

(d) Miscellaneous weight is 5 percent of initial gross weight

The excessively long mission time at the 30-kilowatt power level may be circumvented somewhat by resorting to higher powers. Probably the most conjectural area in any high-power (megawatt range) electric-propelled mission analysis is that of power generation. Firm electrical-generator weight values are indefinite because no space-oriented systems of this size have yet been constructed; however, much can be learned from the specific weight growth experience in the 1- to 30-kilowatt range and about the likelihood of realizing the power-generation weight values that have been used in published analytical mission studies. Specific weight is shown as a function of power level for conceptual designs dating from about 1958 (refs. 57, 60, and 61) and for two recent hardware-development systems (ref. 62, fig. 40). The large decrease in conceptual design specific weight at higher power levels is primarily due to lower unit reactor weight, increased shielding efficiency, and higher cycle temperatures with resultant improved

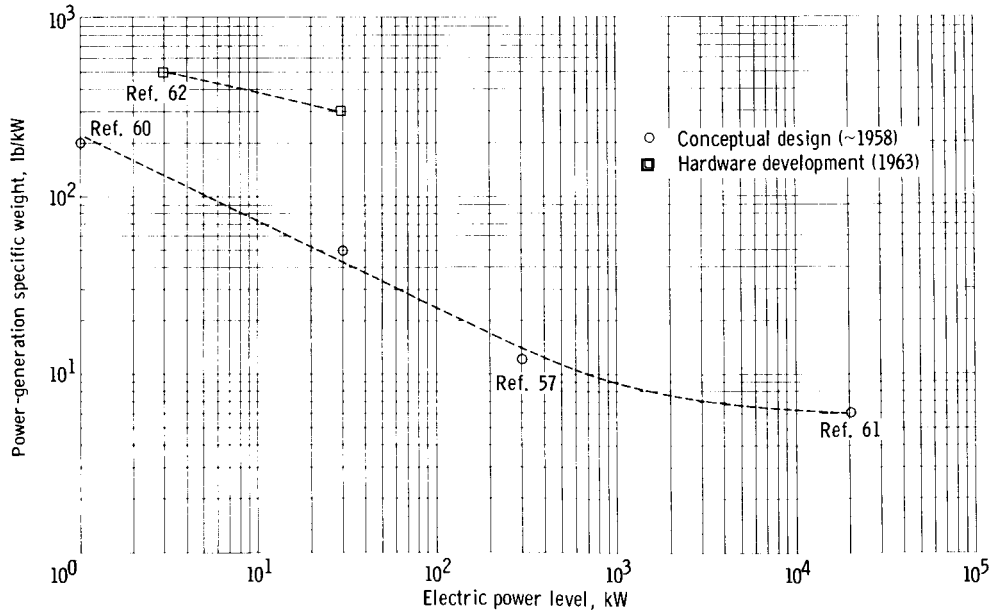

Figure 40. - Specific weight for electric-power generator systems over range of power levels.

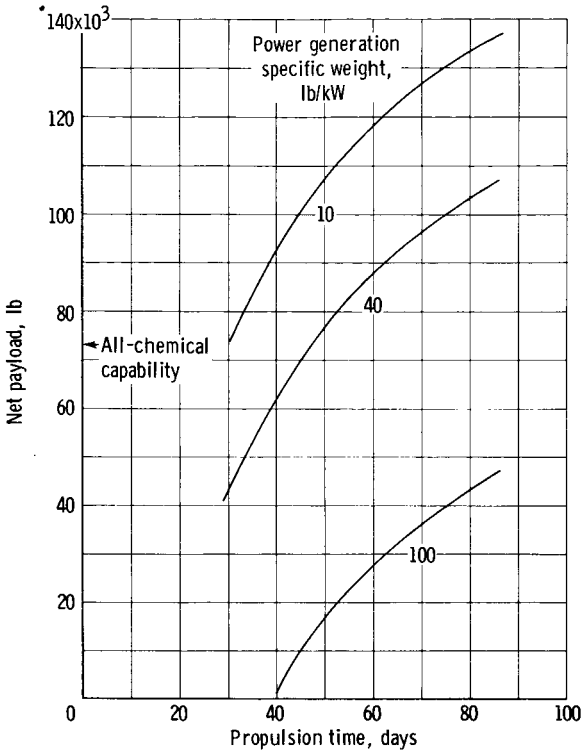

Figure 41. - Effect of electric generator weight on net payload for satellite-raising mission. Booster, Saturn V; arc-jet thrustor, 1 megawatt.

radiator design. Unfortunately, these conceptual generator weights have grown considerably on exposure to experimental development. At the 1-kilowatt power level the specific powerplant weight was calculated to be 200 pounds per kilowatt (ref. 60); at the 30-kilowatt level, 50 pounds per kilowatt; at the 300-kilowatt level, 14 pounds per kilowatt (ref. 57); and at the 20-megawatt level, 7 pounds per kilowatt (ref. 63). These hypothetical values are in sharp contrast to the current developmental weights of 500 pounds per kilowatt at the 3-kilowatt level (ref. 62) and about 296 pounds per kilowatt at the 30-kilowatt level for the SNAP-8 system. It is possible that the conceptual specific powerplant weights will increase even more in the megawatt range than in the kilowatt power range as the hardware stage is approached. The goals are more difficult at the higher power level; for example, the design cycle temperature is raised from the 1500° to 2500° R level. The overall powerplant efficiency is raised from about 5 to 25 percent. At this point then, any specific powerplant weight in the megawatt power range is little more than a guess.

The satellite-raising mission was calculated for the 1-megawatt arc thrustor boosted into a 300-mile orbit with a Saturn V chemical boost stage (fig. 41) for a range of specific generator weights from 10 to 100 pounds per kilowatt. The structure, tankage, and miscellaneous weight assumptions were the same as those used for the 30-kilowatt arc thrustor study. At a raising time of 50 days, the arc-jet thrustor operating with a specific generator weight of 40 pounds per kilowatt is competitive with the all-chemical system. The effect of changes in arc-jet thrustor size on net payload is shown in figure 42 for the same mission at a specific powerplant weight of 40 pounds per kilowatt. For the 0.5-megawatt power level, comparatively good payloads are available, but the mission time is relatively long. Until more is learned about the power-generation specific weights, these curves in figures 41 and 42 are little more than qualitative trends.

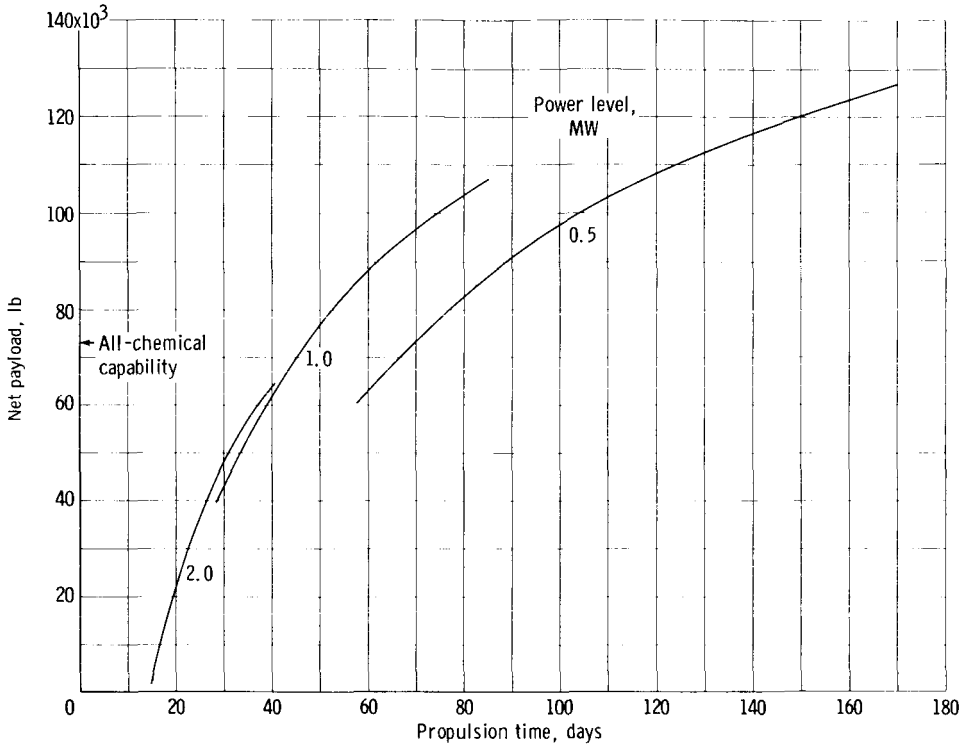

Figure 42. - Effect of power level on net payload for arc-jet thrustor satellite-raising mission. Booster, Saturn V; powerplant specific weight, 40 pounds per kilowatt.

Lunar-Ferry Mission

It has been suggested that the major space mission following the initial lunar landings will be the establishment of a sizable exploration base (ref. 64). Such a supply depot will require extensive cartage between the Earth and the Moon. The means for propelling a lunar ferry has been examined by several analysts in the past (refs. 3, 64, and 65). The arc-jet thrustor comparison with the chemical, nuclear, and ion propulsion means shown in figure 43 is typical of the results of these studies. Although the electric-arc thrustor vehicle is shown to have considerable payload advantage over that available with the Nova class chemical system, the purpose herein is to examine the validity of some basic assumptions that go into these typical lunar-ferry calculations. Three assumptions include: (1) 10 000-hour continuous operation, (2) no biological shield weight for slow traversal of the Van Allen belt, and (3) specific weight for electric power source of 7 pounds per kilowatt.

The term 10 000-hour continuous operation is a frequently used period in many low-thrust space missions; attaining a reasonable degree of reliability for such a long operating time may be a difficult task. Although the present-day science of reliability is comparatively recent (ref. 66) there are enough fundamentals established to permit a first-order reliability assessment of very long operating life for a system (study per-

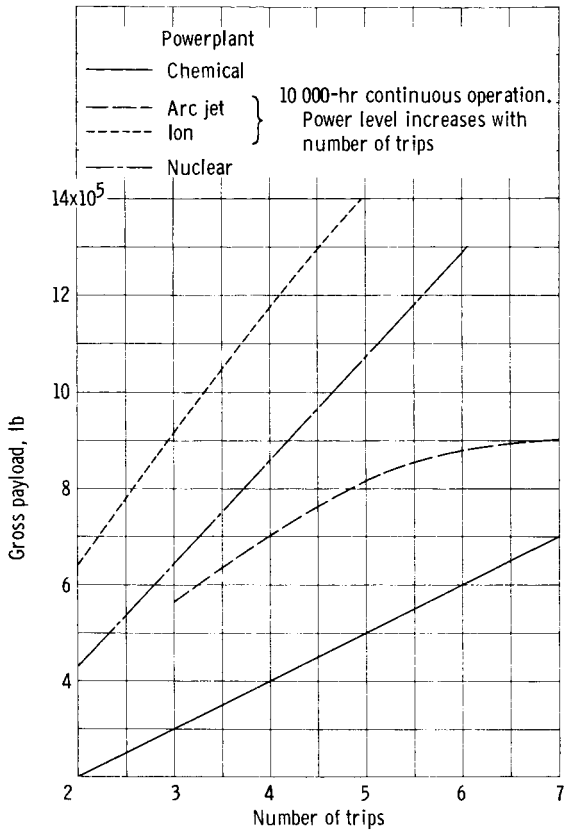

Figure 43. - Gross payload available with various powerplant types used for lunar-ferry mission. Nova size booster with 400 000 pounds per launch in 300-mile orbit (ref. 64).

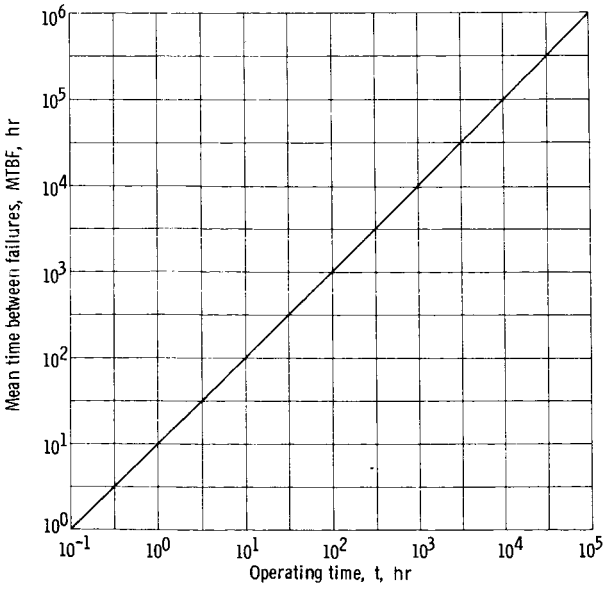

Figure 44. - Relation between required mean time between failures and operating time for a required system reliability of 0. 90.

formed with the advice of Mr. V. R. Lalli of Reliability and Quality Assurance Office of Lewis). One equation that can be used to describe the reliability function is defined as

$$R = e^{-t/m}$$

where

R system reliability

m mean operating time between failures

t mission time

A detailed discussion is given in reference 66.

By use of this equation, the relation between required mean time between failures (MTBF) and operating time for a required system reliability of 0. 90 was computed and is shown in figure 44. The increased operating time for low-thrust compared with that for high-thrust propulsion results in much higher mean time between failures. For example, the chemical rocket in the Atlas-Centaur system may have an engine operating time of about 0. 1 hour with a required MTBF of about 1 hour for 0. 90 reliability; whereas to obtain equal reliability for a system operating time at the 10 000-hour level, the required MTBF is of the order of 100 000 hours. As delineated in reference 66, equipment with such high MTBF is evaluated statistically. This type of data must be used with extreme care as it usually does not account for system stresses in making any comparison. Regardless, it is clear that obtaining anything approaching 0. 90 reliability at 10 000-hour life for electric thrustor systems, where there are moving parts and high tem-

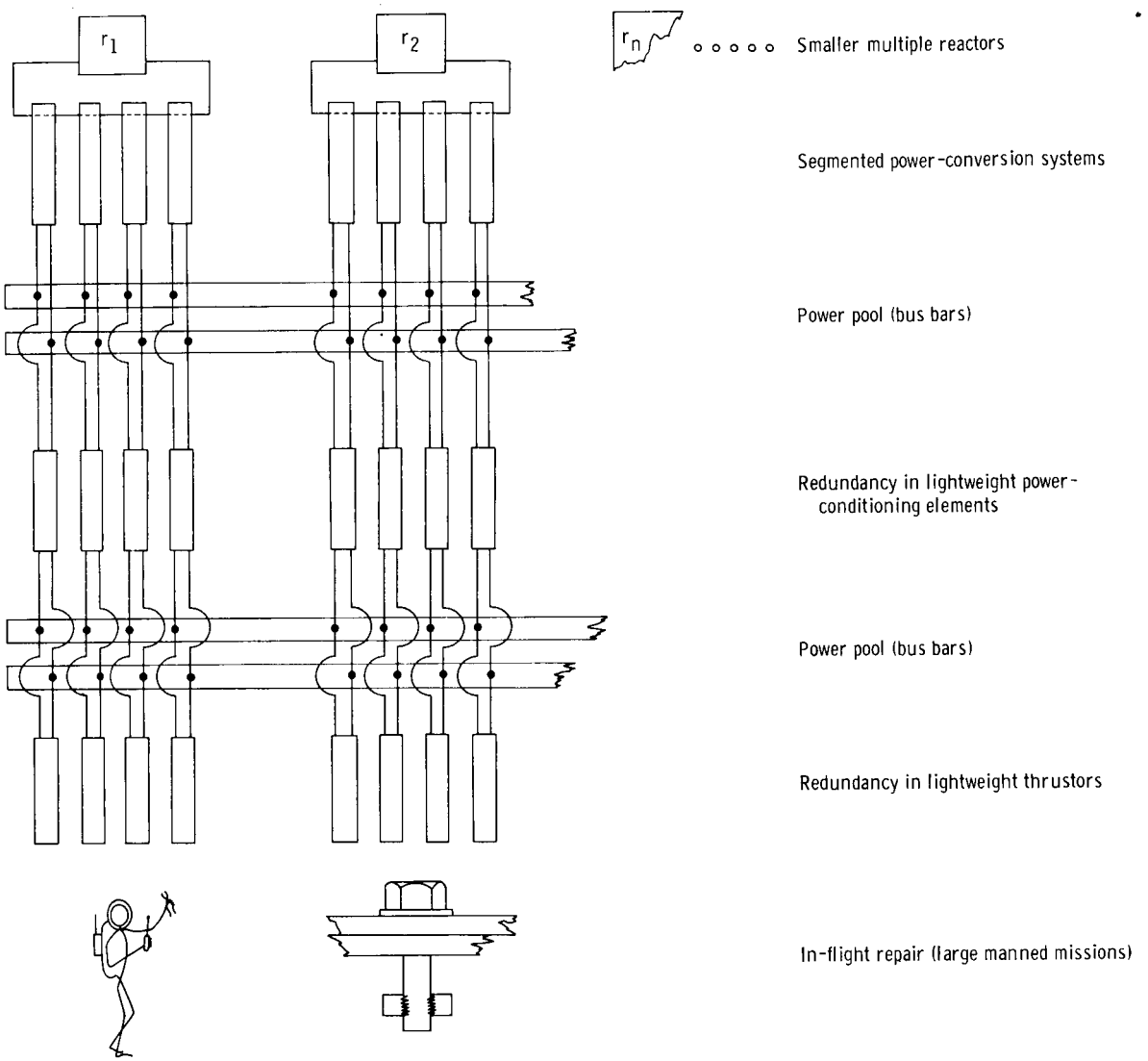

Figure 45. - Design concepts to improve electric-propulsion-system reliability.

peratures, will require considerable effort.

A general discussion of long-life operation with rotating machinery is given in reference 67. Methods for relieving the long-term operation problem for low-thrust propulsion systems are discussed in reference 68; these include multiple engines, segmented engines, power pooling, redundancy, and in-flight repair (see fig. 45). By the use of smaller multiple engines, a single failure may not abort the mission; the lower total power output can be made up by trajectory, impulse, or operating-point adjustments, for example. Segmenting the output of the power source may mean that a failure in a radiator or alternator, for example, will not invalidate the operation of an entire reactor. By pooling the power output of the electrical system, malfunction of an individual unit need not materially change the electrical input to the thrustors. Additional re-

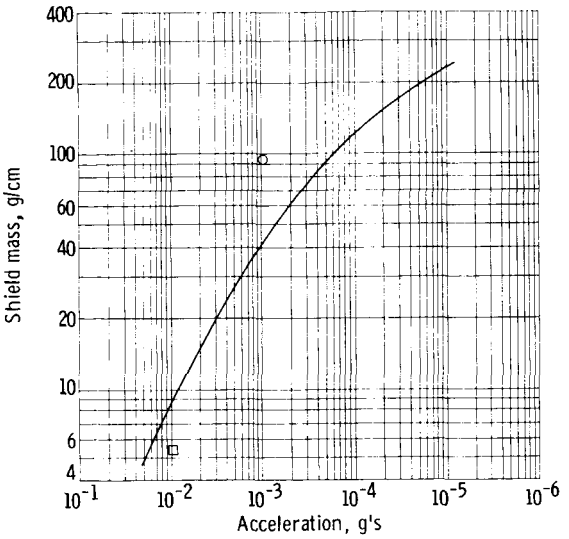

Figure 46. - Biological shield mass required for slow traversal of Van Allen radiation belts (ref. 69).

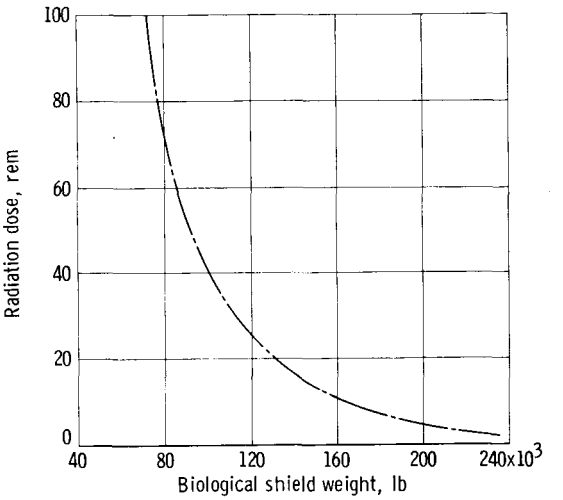

Figure 47. - Biological shield-weight allowance for acceleration of 10^{-4} g's through Van Allen radiation belt (ref. 69).

liability can be afforded by having redundancy in the lightweight components, such as the power-conditioning or thrustor segments. Of course, for the large manned mission, it is generally assumed that some in-flight repair would be possible to correct minor system malfunctions (fig. 45). At any rate it is clear that most of these schemes represent weight additions or added complexity, but they may make possible the reliable 10 000-hour operating life, which might not otherwise be attainable.

Typically, the consideration of biological shielding weight is beyond the scope of the lunar-ferry-mission studies with the low-thrust arc-jet thrustor propulsion (ref. 64). For slow traversal of the Van Allen radiation belt, however, large increases in shield weight are required to prevent excessive radiation levels. This problem is evident from the plot of required shielding mass as a function of acceleration in figure 46. For a ballistic departure from Earth (about 12 min residence in the Van Allen belt) the required shield mass is less than that contained in the vehicle structure. With any electric thrustor, where the required shield mass may be as high as 125 grams per square centimeter (equivalent to about a 2-ft thickness of carbon for 10^{-4} g's acceleration) the required biological shielding thickness can become exceedingly heavy. A direct assessment of the shield weight is shown as a function of radiation dose in figure 47 (ref. 69). For an acute radiation level of 100 rem and an acceleration of 10^{-4} g's, the required shield weight may be in excess of 50 000 pounds, a considerable correction to apply to the lunar payload curves shown in figure 43 for electric propulsion.

Proposals have been made to circumvent the serious biological shield problem by sending the vehicle unmanned (refs. 3, 64, and 65). If this is a prerequisite of the low-thrust vehicle compared with the high-thrust vehicle, however, some not insignificant

penalty arises from not being able to carry a man on board the "slow" lunar transport. In considering the total radiation problem, other hazards, such as solar flares or the nuclear power source, must be evaluated simultaneously. It is possible, for example, that supplying sufficient biological shielding against a giant solar flare may afford sufficient protection for slow traversal of the Van Allen belts (see ref. 69).

Although the calculation procedures and assumptions for the curves presented in figure 43 are detailed in reference 64, some of the conditions bear emphasis. For both low-thrust electric-propulsion systems, the calculation is made for 10 000-hour continuous operation, and the payload curves are for constant specific impulse. Therefore, as the number of lunar trips is increased, the megawatt electric power level is raised to maintain the 10 000-hour total operating time constant. The 5000-second impulse level for the ion thrustor results in somewhat higher power requirements compared with the 1750-second impulse level for the arc-jet thrustor. It is interesting to note that, in addition to the chemical and arc-jet propulsive systems, the ion thrustor and nuclear rocket were also examined for the lunar-ferry mission; both were superior to the arc-jet thrustor. The assumptions for the ion thrustor, however, may be as unrealistic as for the arc-jet thrustor. In making any of the comparisons of the advanced propulsive systems with the chemical rocket it must be remembered that many components are being considered that exist only on paper, whereas the technology for constructing large chemical boosters is now well in hand.

Guidance and Attitude Control

Many satellite systems require some sort of propulsive energy to maintain their position in a predetermined manner. Forces that tend to aggravate the positioning problem include atmospheric drag, oblateness of the Earth, and perturbations from other bodies. Among the many propulsive types available are the monopropellant and bipropellant chemical rockets, the arc-jet thrustor, and the ion thrustor. Simple, reliable guidance means have been successfully used on several space missions; however, what is sought now is primarily weight saving and longer life for the guidance system. From previous studies of attitude-control and station-keeping propulsion, it is possible to make a weight comparison for the 550-pound synchronous-satellite requirements. The bipropellant chemical-rocket, the arc-jet, and the ion-thrustor system weights are detailed in table XIII. The maximum difference between the three guidance methods is less than 10 percent for the hypothetical 1-year mission life. It should be made clear that all these propulsive means are still in the development stage and that system life experiments have not yet been adequately performed. At the same time, there does not appear to be any clear-cut advantage of one system over the other on the basis of these preliminary data

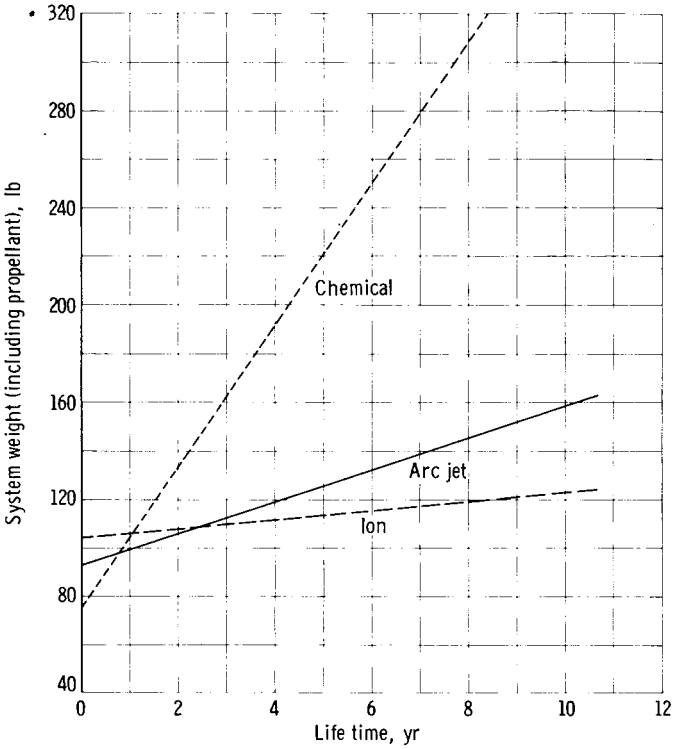

Figure 48. - Weight comparison for three methods of performing station-keeping and attitude-control tasks.

for the 1-year mission life.

That mission life can have an important bearing on guidance-system weight is clearly demonstrated by the curves in figure 48, which is a plot of weight against lifetime. At mission times less than 1 year, the simple and proven chemical system is at a weight advantage over the arc-jet and ion thrustors, primarily because of the heavy solar cells required by the electric rockets. At the 10-year mission life, the highest impulse ion-thrustor system shows considerable promise because the low propellant consumption rate has counteracted the solar electric weight (refs. 70, 71, and 72). A further advantage of the ion-thrustor guidance application is that the negligible propellant consumption permits continuous thrusting, which eases the control problem characteristic of on-off operation (ref. 71).

CONCLUDING REMARKS

In the past several years, considerable progress has been made in the improvement and understanding of the arc-jet thrustor for space propulsion. Engine sizes between the 1- and 200-kilowatt power level have been operated at efficiencies as high as 55 percent. Endurance runs ranging to nearly 500 hours have been performed with uninterrupted operation. Solutions to many of the early operating problems, such as electrode erosion, nozzle cooling, power conditioning, and propellant-feed systems, have been found. Relatively low frozen-flow efficiency at higher impulse levels in the unconstricted-arc designs have been circumvented somewhat by the use of constricted-arc designs that have nonuniform enthalpy profiles. Recently, theories have been advanced to explain, at least partially, the electric-arc operation, about which so little was previously understood. This has enabled the scaling of thrustor size and a reasonable prediction of engine performance. Such a procedure is in sharp contrast to the early history of the arc-jet thrustor, which advanced largely by the "brute force" ex-

perimentation route. Thus, there is now in the conventional arc-jet thrustor a fairly well-developed moderately high-impulse electric engine and in the advanced experimental arc-type thrustors a potential of a high-specific-impulse (10 000 sec) engine.

Next to be examined are the space missions for which this electric drive was proposed several years ago. At the outset, it was recognized that the arc-jet thrustor would be useful for the near-Earth tasks. The 1000- to 2000-second specific-impulse range placed the conventional arc jet between the capabilities of the chemical rocket in the high-thrust area and the ion engine in the low-thrust regime. Three major areas outlined for the arc jet were that of satellite raising, lunar ferry, and attitude control and guidance. The 300-mile to synchronous-orbit mission with smaller payloads has been largely precluded by the large specific weight growth of the SNAP-8 electric-generator system. Practical use of the arc-jet thrustor for the raising mission will depend heavily on the specific weight of the electric power source. At the 40 pound per kilowatt specific powerplant weight, the arc jet may be competitive with the C-5 chemical boost system. Of course, if the nature of the electrical power source needed for a particular mission coincides with power requirements of the thrustor and if operating life is not a problem, any propulsion comparison would have to be weighed accordingly.

The considerable radiation problem associated with slow traversal of the Van Allen belts, the difficult reliability problem associated with 10 000-hour continuous operation, and the lack of a power source in the megawatt range at anywhere near the early specific weight numbers are some prominent liabilities associated with the arc jet for the lunar ferry mission. Still, one might say there will be much progress in the areas of shielding and power generation in the next decade or two. Unfortunately, looking into the future probably finds more promise in either the nuclear rocket or the ion thrustor than in the arc-jet engine for the lunar transport.

The attitude and guidance control of satellites is not without merit for the arc thrustor, although the proven chemical rocket is probably the lightest of all engines for the short-term mission (less than 1 yr). For long lasting trips (in excess of 3 yr) the low fuel rate of the high specific impulse ion thrustor makes it a difficult competitor for this mission, although long-term life remains to be demonstrated.

In conclusion, the arc-jet thrustor is now a fairly well-developed engine, but mission applications will not arise unless low-specific-weight electric-generating systems are developed.

Lewis Research Center,
National Aeronautics and Space Administration,
Cleveland, Ohio, December 17, 1964.

REFERENCES

1. Mickelson, William R.: Electric Propulsion for Space Flight. Aerospace Eng., vol. 19, no. 11, Nov. 1960, pp. 6-11; 36-52.

2. Ehricke, K. A.: Comparison of Propulsion Systems: Solar Heating, Arc Thermodynamics and Arc Magnetohydrodynamics. Proc. Advanced Propulsion Systems Symposium, Pergamon Press, 1959, p. 71.

3. Camac, M.; Kantrowitz, A. R.; Petschek, H. B.: Plasma Propulsion Devices for Space Flight. Res. Rept. No. 45, AVCO Res. Lab., Feb. 1959.

4. Giannini, Gabriel M.: The Arc Jet. Paper Presented at Second Symposium on Advanced Propulsion Concepts, ARDC and Avco Corp., Boston (Mass.), Oct. 7-8, 1959.

5. Evvard, J. C.: Electric Space Propulsion. Elec. Eng., vol. 79, no. 7, July 1960, pp. 555-562.

6. Froehlich, J. E.: Capabilities of Multistaged Chemical Rocket Systems. Astronautica Acta, vol. 6, no. 6, 1960, pp. 311-321.

7. Luidens, Roger W.: Manned Mars Landing Mission via High Thrust Rockets. Manned Planetary Mission Technology Conference, NASA TM X-50123, 1963, pp. 15-30.

8. Spencer, Dwain F., et al: Nuclear Electric Spacecraft for Unmanned Planetary and Interplanetary Missions. Rept. No. 32-281, Jet Prop. Lab., C. I. T., Apr. 25, 1962.

9. Heller, Gerhard: Study of Arc Jet Propulsion. Paper No. 1748-61, ARS, 1961.

10. John, Richard R.; and Bade, William L.: Recent Advances in Electric Arc Plasma Generation Technology. ARS J., vol. 31, no. 1, Jan. 1961, pp. 4-17.

11. John, R. R., et al.: Energy Addition and Loss Mechanisms in the Thermal Arc Jet Engine. Paper No. 63-022, AIAA, 1963.

12. Rosenbaum, Burt M.; and Levitt, Leo: Thermodynamic Properties of Hydrogen from Room Temperature to 100, 000° K. NASA TN D-1107, 1962.

13. Bray, K. N. C.: Atomic Recombination in a Hypersonic Wind-Tunnel Nozzle. J. Fluid Mech., vol. 6, pt. I, July 1959, pp. 1-32.

14. Oswalt, Lawrence R.; and Widawsky, Arthur: Investigation of Exhaust Nozzle Flow Phenomena in Arc-Jet Engines. Rept. No. 25052, The Marquardt Corp., May 31, 1962.

15. Jack, John R.: Theoretical Performance of Propellants Suitable for Electrothermal Jet Engines. NASA TN D-682, 1961.

16. Schaefer, John W.; and Ferrante, John: Analytical Evaluation of Possible Noncryogenic Propellants for Electrothermal Thrustors. NASA TN D-2253, 1964.

17. Shapiro, Ascher H.: The Dynamics and Thermodynamics of Compressible Fluid Flow. Vol. 1. Ronald Press Co., 1953.

18. John, R.R., et al.: Theoretical and Experimental Investigation of Arc Plasma-Generation Technology. Rept. No. ASD-TDR-62-729, Pts. I-II, Vols. 1-2, Avco Corp., 1963.

19. John, R.: Thirty Kilowatt Plasmajet Rocket-Engine Development. Rept. No. RAD TR-64-6, Avco Corp., July 15, 1964.

20. Stine, Howard A.; and Watson, Velvin R.: The Theoretical Enthalpy Distribution of Air in Steady Flow Along the Axis of a Direct-Current Electric Arc. NASA TN D-1331, 1962.

21. John, R.R.; Bennett, S.; Connors, J.F.; and Enos, G.: Thermal Arc Jet Research. Rept. No. ASD-TDR-63-717, Avco Corp., June 1963.

22. Finkelnberg, W.; and Maecker, H. (B. Eckstein, trans.): Electric Arcs and Thermal Plasmas. Aeronautical Res. Lab., Jan. 1962.

23. Jack, John R.; and Schaefer, John W.: Possible Effects of Nonuniform Flows on Performance of Electrothermal Thrustors. NASA TN D-1732, 1963.

24. John, R.: Thirty-Kilowatt Plasmajet Rocket Engine Development. Rept. No. RAD-SR-61-182, Avco Corp., Nov. 29, 1961.

25. Cann, G.L.; Moore, R.A.; Buhler, R.D.; and Marlotte, G.L.: Thermal Arc Jet Research. Rept. No. ASD-TDR-63-632, Electro-Optical Systems, Inc., Aug. 15, 1963.

26. Shepard, C.E.; and Watson, V.R.: Performance of a Constricted-Arc Discharge in a Supersonic Nozzle. Paper No. 63-380, AIAA, 1963.

27. Anon.: Thirty-Kilowatt Plasmajet Rocket-Engine Development. Third Year Development Program, QPR-2, Rept. No. RAD SR-63-244, Avco Corp., Dec. 1963.

28. McCaughey, O.J.: Development of a Plasmajet Rocket Engine for Attitude and Orbit Control. Rept. No. FR-112-651, Plasmadyne Corp., June 1964.

29. John, R.R.; Bennett, S.; Chen, M.; and Connors, J.F.: Arc Jet Engine Performance Experiment and Theory, V. Paper No. 2667-62, ARS, 1962.

30. Anon.: Research and Advanced Development of a 2 kw Arc-Jet Thrustor. Rept. No. 1FR113-2521, Plasmadyne Corp., Nov. 15, 1963.

31. Todd, J. P.: Thirty KW Arc-Jet Thrustor Research. Rept. No. FR024-10338 (APL-TDR-64-58), Giannini Scientific Corp., Mar. 1964.

32. Richter, R.: Development of a 30 KW Three-Phase AC Arc Jet Propulsion System. (NASA CR-54112), General Electric Co., Aug. 4, 1964.

33. Richter, R.: Study of AC Arc Dynamics, Stabilization, and Starting Criteria. Rept. No. GE-63, FPD283, General Electric Co., July 1963.

34. Greco, Robert V.; and Stoner, Willis A.: Development of a Plasmajet Rocket Engine for Attitude Control. Rept. No. GRC 1341-A (FR-111-651), Plasmadyne Corp., Dec. 1, 1961.

35. John, R. R.; Connors, J. F.; and Bennett, S.: Thirty-Day Endurance Test of a 30 KW Arc Jet Engine. Paper No. 63-274, AIAA, 1963.

36. John, R. R.: Thirty-Kilowatt Plasmajet Rocket-Engine Development. Rept. No. RAD SR-62-255, Avco Corp., Dec. 1962.

37. Anon.: Thirty-Kilowatt Plasmajet Rocket Engine Development. QPR-1, June-Aug. 1963, Avco Corp., Sept. 1963.

38. John, R. R.: Thirty-Kilowatt Plasmajet Rocket-Engine Development. Rept. No. RAD SR-62-182, Avco Corp., Sept. 11, 1962.

39. Anon.: Thirty-Kilowatt Plasmajet Rocket Engine Development. Rept. No. RAD SR-64-80, QPR 3, AVCO Corp., Mar. 1964.

40. Ducati, Adriano C.; Giannini, Gabriel M.; and Muehlberger, Erich: Experimental Results in High-Specific-Impulse Thermo-Ionic Acceleration. AIAA J., vol. 2, no. 8, Aug. 1964, pp. 1452-1455.

41. Girouard, H.; Graber, F. M.; and Myers, B. F.: Catalysis of Hydrogen Atom Recombination. Rept. No. AE63-0078, General Dynamics/Astronautics, Feb. 12, 1963.

42. Noeske, H. O.; and Kassner, R. R.: Research of a Bipropellant Plasmajet Device. Rept. No. R-3524, Rocketdyne Div., North Am. Aviation, Inc., Apr. 1962.

43. Ghay, Mark: Double Arc Feasibility. Space Dynamics Corp., 1965.

44. Williams, James C.; Wilber, Paul C., III; and Chuan, Raymond L.: Analytical Study of the Heating of Hypersonic Air Flow by Electrode-Less High-Frequency Discharge. Rept. No. TR 59-23, Arnold Eng. Dev. Center, Oct. 1959.

45. John, R. R.: Thirty-Kilowatt Plasmajet Rocket Engine Development. Rept. No. RAD-SR-64-168, QPR 4, Avco Corp., June 1964.

46. Anon.: Experimental and Analytical Investigations of Crossed-Field Plasma Accelerators. Rept. No. ASD-TDR-63-307, Northrop Space Labs., May 1963.

47. Blackman, V. H.; and Sunderland, R. J.: The Experimental Performance of a Crossed-Field Plasma Accelerator. Paper No. 2633-62, ARS, 1962.

48. Bernatowicz, D., et al.: Space Electrical Power. Astronautics and Aerospace Eng., vol. 1, no. 4, May 1963, pp. 22-117.

49. Boehme, R. J.; and Cagle, E. H.: Power Source for a 1-kw Arc Engine Test Capsule. AIAA J., vol. 1, no. 5, May 1963, pp. 1168-1169.

50. Page, Russell J.; and Humpal, Harold: Objectives and Design of a 1-kw Arc-Jet Engine for Space Flight Testing. Prog. in Astronautics and Aeronautics, vol. 9, Academic Press, Inc., 1963, pp. 3-20.

51. Fowle, A. A.: Cryogenic Propellant Feed Systems for Electrothermal Engines. Rept. No. C-64470, Arthur D. Little, Inc., Jan. 1963.

52. Barclay, R. B.; Singleton, A. H.; and Stelts, P. D.: Propellant Storage and Transfer Systems for Electrothermal Engines. Air Products and Chem., Inc., Nov. 8, 1962.

53. Anon.: Development of Thermal Protection System for a Cryogenic Spacecraft Module. Rept. No. LMSC H703794, Lockheed Missiles and Space Systems, Oct. 15, 1964.

54. Roos, G. E., et al.: Electrothermal Engine Propellant Storage and Feed System Study Phase II Report. Rept. No. 13558, Beech Aircraft Corp., Sept. 7, 1962.

55. Anon.: Propellant Feed Systems for Electrothermal Engines. Garrett Corp., Mar.-Nov., 1962.

56. Evvard John C.: How Much Future for Electronic Propulsion? Astronautics and Aerospace Eng., vol. 1, no. 7, Aug. 1963, pp. 92-97.

57. Schwartz, Ira R.; and Stuhlinger, Ernst: The Role of Electric Propulsion in Future Space Programs. Paper No. 2654-62, ARS, 1962.

58. Yarymovych, M. I.; deWiess, F. A.; and John, R. R.: Feasibility of Arcjet Propelled Spacecraft. Astronautics, vol. 7, no. 6, June 1962, pp. 36-42.

59. Marchaud, F. E.; and McCaughey, O. V.: Applicability of Electrothermal Arc Jet Engines for Attitude Control and Station Keeping of a 550 Pound Synchronous Equatorial Satellite. Plasmadyne Corp., Feb. 1963.

60. Huth, J. H.: Space Vehicle Power Plants. Rept. No. P-1861, Rand Corp., Dec. 22, 1959.

61. Skifstad, J. G.: Summary of Published Literature Concerned with Electric Arc Phenomena Pertinent to Plasma Jet Devices. Rept. No. TM 62-4, Purdue Univ., Aug. 1962.

62. Anderson, G. Montgomery: Nuclear Reactor Systems. Astronautics and Aerospace Eng., vol. 1, no. 4, May 1963, pp. 27-36.

63. English, Robert E.; Slone, Henry O.; and Bernatowicz, Daniel T.; Davison, Elmer H.; and Lieblein, Seymour: A 20,000-Kilowatt Nuclear Turboelectric Power Supply for Manned Space Vehicles. NASA 2-20-59E, 1959.

64. Brown, Harold; and Nicoll, Harry E., Jr.: Electrical Propulsion Capabilities for Lunar Exploration. AAIA J., vol. 1, no. 2, Feb. 1963, pp. 314-319.

65. London, Howard S.: A Study of Earth-Satellite to Moon-Satellite Transfers Using Non-Chemical Propulsion Systems. Rept. No. R-1383-1, United Aircraft Corp., May 21, 1959.

66. Carroll, John M.: Mathematics of Reliability. Electronics, vol. 35, Nov. 30, 1962, pp. 54-59.

67. Kovacik, Victor P.: Dynamic Energy Conversion. Astronautics and Aerospace Eng., vol. 1, no. 4, May 1963, pp. 84-88.

68. Pinkel, B., et al.: A Consideration of the Problems Relating to Feasibility, Utility, and Development of Electrical Propulsion Systems. Memo. R. M. 3469, Rand Corp., Sept. 1963.

69. Wallner, Lewis E.; and Kaufman, Harold R.: Radiation Shielding for Manned Space Flight. NASA, TN D-681, 1960.

70. Molitor, Jerome H.: Ion Propulsion for the Control of Stationary Satellites. Paper No. 2666-62, ARS, 1962.

71. Boucher, Roland A.: Electrical Propulsion for Control of Stationary Satellites. Jour. Spacecraft and Rockets, vol. 1, no. 2, Mar.-Apr. 1964, pp. 164-169.

72. Moeckel, W.; Baldwin, L.; English, R.; Lubarsky, B.; and Maslen, S.: Satellite and Space Propulsion Systems. TN D-285, 1960.

TABLE I. - PERFORMANCE OF 1-KILOWATT ARC JET WITH VARIOUS PROPELLANTS

Propellant	Power, W	Weight flow rate, lb/sec	Voltage, V	Current, A	Thrust, lb	Specific impulse, sec	Efficiency, percent	Test time, hr	Life expectancy, hr
Ammonia	920	1.10×10^{-5}	59	15	0.006	550	8	2	1
Nitrogen	550	2.75	40	13	.009	350	13	2	1
Helium	370	1.00	30	12	.005	550	17	2	1
Argon	130 - 300	2.00 - 5.70	18 - 20	9.5 - 15	----	80	3	Short	Short
Lithium hydride	700	----------	70	10	----	400 - 800	8 - 12	Short	Short

TABLE II. - PERFORMANCE OF 30-KILOWATT ARC JET WITH HYDROGEN (REFS. 36, 37, and 45)

Test time, hr	Mass flow rate, g/sec	Voltage, V	Current, A	Thrust, g	Specific impulse, sec	Efficiency, percent
110	0.14	170	175	182	1300	37.7
250	.16	198	151	211	1300	44.6
10	.10	131	229	151	1510	36.7
46	.12	---	---	180	1500	44

TABLE III. - TYPICAL OPERATING ENVELOPES FOR AN AMMONIA AND A HYDROGEN ARC JET (REF. 38)

Mass flow rate, g/sec	Current, A	Voltage, V	Thrust, g	Specific impulse, sec	Efficiency, percent
Hydrogen					
0.244	186	161	246	1008	41.2
.230	191	158	240	1042	39.7
.218	192	155	232	1063	39.7
.204	200	152	224	1096	38.7
.190	203	148	215	1131	38.8
.177	210	145	208	1174	38.7
.164	210	143	202	1232	39.8
.150	222	138	192	1280	38.5
Ammonia					
0.50	250	122	299	597	28.1
.45	255	118	288	640	29.4
.40	260	116	277	692	30.6
.38	260	115	272	715	31.3
.36	262	115	268	742	31.8
.34	265	114	265	780	33.0
.32	270	112	262	819	34.1
.30	270	112	260	866	35.8
.28	270	111	254	910	36.8
.26	275	110	252	970	38.8
.24	288	106	243	1012	38.6

TABLE IV. - THIRTY-KILOWATT ALTERNATING-CURRENT ENGINE PERFORMANCE FOR HYDROGEN (REF. 32)

[Test time, 1 hr 42 min.]

Power, kW	Current, A	Mass flow rate, g/sec	Thrust, g	Specific impulse, sec	Efficiency, percent
27.0	105	0.227	224	988	40.0
26.9	110	.227	224	988	40.1
29.5	116	.227	236	1040	40.6
30.0	119	.227	237	1046	40.3

TABLE V. - PERFORMANCE OF RADIATION-COOLED HIGH-POWER HYDROGEN ARC JET (REF. 37)

Arc power, kW	Current, A	Voltage, V	Mass flow rate, g/sec	Thrust, g	Specific impulse, sec	Efficiency, percent
150	928	162	0.413	660	1600	33.7
151	928	163	.396	650	1640	33.9
151	928	163	.376	640	1702	34.6
153	948	162	.347	635	1830	36.4
153	964	159	.327	630	1925	38.1
173	1080	160	.327	660	2080	37.0
198	1232	161	.327	693	2120	35.6
216	1350	160	.327	724	2210	35.6

TABLE VI. - PERFORMANCE OF PRELIMINARY INVESTIGATION OF HIGH-SPECIFIC-IMPULSE ARC THRUSTOR (REF. 39)

Mass flow rate, g/sec	Current, A	Potential, V	Power, kW	Thrust, g	Efficiency, percent	Specific impulse, sec	Chamber pressure, mm Hg
0.050	1560	69	108	136	16.5	2720	50
.050	2210	76	167	221	28	4420	50
.026	2360	82	196	192	35	7400	14

TABLE VII. - PERFORMANCE OF THERMAL ARC JET (REF. 40)

Mass flow rate, g/sec	Power, kW	Thrust, g	Efficiency, percent	Specific impulse, sec	Enthalpy, Btu/lb
0.025	103	105	20	4 200	1.2×10^6
.025	190	180	33	7 200	2.2
.025	260	250	46	10 000	3

TABLE VIII. - BEST PERFORMANCE OF THERMAL

ARC JET WITH HYDROGEN

Power, kW	Specific impulse, sec	Thrust, g	Efficiency, percent	Test time	Type of test	Comments
1	1 100	4.5	35	25 hr	Continuous (ref. 34)	Average over first 12 hr; decayed rapidly afterwards
2	935	13.6	30	150 hr	Continuous (ref. 30)	
30	1 010	250	41	720 hr	Interrupted (ref. 35)	Terminated voluntarily; thrustor in excellent condition
30	1 010	338	54	500 hr	Continuous (ref. 31)	
30	1 320	211	44	250 hr	Continuous (ref. 37)	
30	1 520	180	44	46 hr	Interrupted (ref. 45)	
[a]30	1 020	230	38	250 hr	Interrupted (ref. 32)	Performance was not verified throughout test
200	2 120	693	35	10 min	Data point (ref. 37)	
127 168	5 900 10 100	148 137	31 40	50 hr 50 hr	Continuous Continuous	Water cooled; not conventional arc jet

[a]Alternating current.

TABLE IX. - ARC-JET PERFORMANCE FOR HYDROGEN

WITH POWER APPLIED TO ACCELERATOR

Accelerator power, kW	Magnetic-field strength, G	Accelerator current, A	Thrust, g	Specific impulse, sec	Mass flow rate, g/sec (a)	Total power, kW	Overall efficiency, percent
0	0	0	108	900	0.12	25	18.6
10.4	0	200	108	900	.12	35.4	13.1
23.0	1000	200	157	1310	.12	48.0	20.6
30.0	1500	200	181	1510	.12	55.0	23.8
34.2	2000	185	200	1670	.12	59.2	27.1
72.0	2500	400	212	2120	.10	102.0	21.2

[a]Ref. 38.

TABLE X. - THIRTY-KILOWATT SNAP-8 ELECTRIC

SYSTEM WEIGHTS GROWTH

Component	Conceptual design weight, lb (a)	Component	Developmental system weight, lb (b)
Reactor	373	Reactor	550
Shield	364	Shield	1840
Contingency	160	Radiation	2781
Power conditioning	667	Power conditioning	2974
		Radiator structure[b]	809
Total	1564		
		Total	8894

[a]Aerojet General Proposal to NASA "Nuclear Power Conversion System," Table 2-1, December 1959.

[b]Private communication with H. O. Slone of SNAP-8 Project Office, Lewis Research Center.

TABLE XI. - ELECTROTHERMAL STORAGE AND

FEED SYSTEMS FOR 30-KILOWATT ENGINE

	Hydrogen	Ammonia
Specific impulse, sec	1000	750
Mass flow rate, lb/sec	5.0×10^{-4}	8.8×10^{-4}
Propulsion time, days	85	60
Method of storage	Subcritical	Liquid phase
Tank material, percent	5 Al	5 Al
	2.5 Sn	2.5 Sn
	92.5 Ti	92.5 Ti
Tank configuration	Cylindrical with hemispherical ends	Toroid
Outside diameter, ft	9.5	3.33, 10.0
Maximum design pressure, lb/sq in. abs	35	100
Overall length, ft	16.2	---
Tank skin thickness, in.	0.013	0.045
Total heat leak, Btu/hr	177	-----
Weight of propellant, lb	3885	4740
Weight of storage system (less propellant), lb	603	433
Total weight, lb	4488	5173

TABLE XII. - ELECTROTHERMAL STORAGE AND FEED SYSTEMS FOR 1-KILOWATT ENGINE

	Hydrogen	Ammonia
Specific impulse, sec	1000	750
Mission time, yr	3	3
Mass flow rate, lb/sec	1.0×10^{-5}	1.43×10^{-5}
Propulsion cycles	9.45×10^{-5}	---
Storage method	Subcritical	Liquid-phase
Tank material, percent	5 Al	6 Al
	2.5 Sn	4 V
	92.5 Ti	90 Ti
Tank configuration	Sphere	Sphere
Outside diameter, ft	2.17	1.18
Maximum design pressure, lb/sq in. abs	50	480
Tank skin thickness, in.	0.008	0.020
Total heat leak, Btu/hr	0.458	---
Weight of propellant, lb	20.0	27.5
Weight of storage system (less propellant), lb	22.07	7.12
Total weight, lb	42.07	34.62

TABLE XIII. - WEIGHT COMPARISON FOR ATTITUDE-CONTROL AND STATION-KEEPING PROPULSION

	Bipropellant chemical rocket (a)	Ion thrustor (b)	Arc-jet thrustor (b)
	Weight, lb		
Basic control system	75	41.0	67.5
Propellant	87	6.0	19.0
Solar cells	0	17.5	5.6
Batteries	0	45.5	19.6
Total	162	110.0	111.7

[a]Unpublished data obtained by R. J. Cybulski of Lewis. System design predicated on obtaining 0.003138 lb-sec/pulse.

[b]Ref. 59.